

Development of targeted therapies against FET oncogene sarcomas

Christoffer Vannas

Department of Laboratory medicine
Institute of Biomedicine
Sahlgrenska Academy, University of Gothenburg



UNIVERSITY OF GOTHENBURG

Gothenburg 2025

Cover illustration: Fluorescent cell lines by Christoffer Vannas

© Christoffer Vannas 2025
christoffer.vannas@gu.se

ISBN 978-91-8115-354-5 (PRINT)
ISBN 978-91-8115-355-2 (PDF)

Printed in Borås, Sweden 2025
Printed by Stema Specialtryck AB

När man följer solens nedgång över kanten
Blir man varse att där inte finns nån kant
Förr fanns ett stup långt där ute i Atlanten,
Man trodde skeppen skulle störta ned dess brant.

Och de som vågade hävda annorlunda
Fick härda ut både spott och spe och död.
Så att de andra kunde fortsätta blunda
När solen sjönk och vår himmel färgats röd

Om man istället för att vara så säker
Sträcker sig bortom sin kunskaps horisont.
Då kan man önska att en blidhet nog läker
där nedom kanten vid det oupptäcktas front

Johanna Sand, "Paradigm" från diktsamlingen Upptäcktsfärd

Development of targeted therapies against FET oncogene sarcomas

Christoffer Vannas

Department of Laboratory medicine, Institute of Biomedicine
Sahlgrenska Academy, University of Gothenburg
Gothenburg, Sweden

ABSTRACT

FET oncogene sarcomas are fusion-driven malignancies characterized by gene fusions involving one of the genes *FUS*, *EWSR1* or *TAF15*, fused to a transcription factor partner. FET oncogene sarcomas comprise more than ten different sarcoma entities, with myxoid liposarcoma (MLS) and Ewing sarcoma (EWS) being the most prevalent. Current treatments for advanced disease in MLS and EWS rely on chemotherapy, but outcomes remain poor. New therapies and improved methods to assess treatment efficacy are urgently needed. The aim of this project was to explore potential targeted therapies in preclinical models of MLS and EWS.

Initially, we analyzed receptor tyrosine kinase (RTK) signaling in MLS and tested the efficacy of targeted RTK inhibitors. Overall, they showed limited therapeutic benefit, likely due to compensatory crosstalk between different RTKs facilitated by the chaperone protein HSP90. We subsequently evaluated the HSP90 inhibitor 17-DMAG in both MLS cell lines and a patient-derived xenograft (PDX) model of MLS, observing potent anti-tumor effect. Various HSP90 inhibitors then demonstrated comparable efficacy *in vitro*, while the *in vivo* effects varied significantly between inhibitors. Next, we investigated tumor vessel formation in MLS and found that the tumor vasculature was enriched with pericytes. Additionally, we observed increased PDGFB-PDGFRB signaling, suggesting the presence of an autocrine loop that may influence both cell survival and vascular architecture. Targeting PDGFRB with the multi-RTK inhibitor imatinib caused tumor regression *in vivo*, though it did not noticeably alter the vascular morphology. We then pursued another treatment strategy targeting epigenetic dysregulation caused by the FET fusion oncoproteins. Combined inhibition of BRD4 and histone deacetylases, both epigenetic proteins, resulted in synergistic effects *in vitro* and significant tumor regression *in vivo*. Finally, we explored the use of circulating tumor DNA and inflammatory protein profiles as informative blood-based biomarkers for treatment monitoring. We demonstrated that simultaneous ctDNA and inflammatory protein quantification can be used to monitor treatment response and provide complementary tumor-related data in a patient with metastatic undifferentiated pleomorphic sarcoma.

In conclusion, our findings add to the understanding of dysregulated signaling pathways in FET oncogene sarcomas and potential targeted therapies to be further evaluated in clinical trials. Furthermore, incorporating quantification of novel blood-based biomarkers may enhance the precision and adaptability of

future clinical trials, ultimately improving patient outcomes through real-time response assessment.

Keywords: Myxoid liposarcoma, Ewing sarcoma, FET fusion oncogenes, Precision medicine, tyrosine kinase inhibitors, angiogenesis, epigenetic drugs, liquid biopsy, circulating tumor DNA

ISBN 978-91-8115-354-5 (PRINT)

ISBN 978-91-8115-355-2 (PDF)

SAMMANFATTNING PÅ SVENSKA

Sarkom är en ovanlig familj av cancersjukdomar som utgår från kroppens stödjevävnader och utgör ungefär 1% av alla cancerfall hos vuxna. Vi studerar en specifik grupp av sarkom, som kallas för FET-onkogensarkom. De drivs av genetiska förändringar som kallas för fusionsonkogener, vilka innehåller en av generna *FUS*, *EWSR1* eller *TAF15* som slagits samman med en annan gen. Utöver fusionsonkogenerna har dessa tumörer få andra genetiska förändringar, vilket gör dem till bra modeller för att studera tumörbiologi. De vanligaste sarkomen i den här familjen är myxoida liposarkom (MLS) och Ewing sarkom (EWS). Vid metastaserad sjukdom behandlas båda dessa sjukdomar med tuffa cellgiftsbehandlingar, dessvärre oftast med begränsad framgång. Genom vår kunskap om hur dessa tumörer uppstår har vi i detta projekt utvärderat nya kandidater till målriktade läkemedelsbehandlingar. Vi har odlat och behandlat tumörceller med potentiellt intressanta läkemedel. Genom att utvärdera andelen avdödade tumörceller samt påverkan på protein- och genuttryck efter behandling har vi studerat hur behandlingarna fungerar och vilka läkemedelskombinationer som fungerar bäst. Dessa läkemedel har vi utvärderat vidare i musmodeller av MLS och EWS, för att förstå hur behandlingarna fungerar i levande organismer. Vi fann att läkemedel som hämmar överaktiva tillväxtstimulerande signalvägar i MLS inte hade någon tumörhämmande effekt i odlade tumörcellinjer. Den bristande effekten berodde på ett protein som heter HSP90. Vi observerade att läkemedlet 17-DMAG, som hämmar HSP90, uppvisade lovande effekt vid behandling av både odlade tumörcellinjer och musmodeller av MLS. Andra HSP90-hämmare visade liknande effekt mot odlade tumörcellinjer, men minskade inte tumörtillväxt i musmodeller av MLS. Vi studerade även läkemedel som påverkar blodkärlstillväxt, och observerade en tumörkrympande effekt vid behandling av MLS. Därefter undersökte vi effekten av läkemedel som påverkar epigenetiska processer, dvs hur cellernas DNA packas och regleras, i både MLS och EWS. Vi observerade att en kombination av två epigenetiska läkemedel som hämmar proteinerna BRD4 och histondeacetylaser visar mycket lovande effekt. Till sist har vi gjort en fallstudie på en patient med pleomorft odifferentierat sarkom, där vi studerat hur man genom mätning av blodbaserade biomarkörer kan utvärdera behandlingsrespons. De biomarkörer vi använde oss av var en kombination av DNA-molekyler utgående från tumörceller samt inflammatoriska proteiner. Dessa markörer kan även användas på patienter med FET-onkogensarkom. Sammantaget visar vår forskning att ökad kunskap om tumördrivande processer kan underlätta

utvecklingen av målriktade behandlingar. Vi har identifierat läkemedel med lovande effekt, som nu kan utvärderas vidare i kliniska prövningar för patienter med FET-onkogensarkom. Genom att använda blodbaserade biomarkörer för att övervaka patienterna kan behandlingsutvärdering förbättras, vilket kan underlätta både framtida läkemedelsstudier och uppföljning av patienter i klinisk rutin.

LIST OF PAPERS

- I. **HSP90 inhibition blocks ERBB3 and RET phosphorylation in myxoid/round cell liposarcoma and causes massive cell death *in vitro* and *in vivo***
Safavi S, Järnum S, **Vannas C**, Udhane S, Jonasson E, Tesan Tomic T, Grundevik P, Fagman H, Hansson M, Kalender Z, Jauhiainen A, Dolatabadi S, Wessel Stratford E, Myklebost O, Eriksson M, Stenman G, Schneider Stock R, Ståhlberg A and Åman P
Oncotarget 2016; DOI: 10.18632/oncotarget.6336.
- II. **Different HSP90 Inhibitors Exert Divergent Effect on Myxoid Liposarcoma *In Vitro* and *In Vivo***
Vannas C, Andersson L, Dolatabadi S, Ranji P, Lindén M, Jonasson E, Ståhlberg A, Fagman H and Åman P
Biomedicines 2022; DOI: 10.3390/biomedicines10030624
- III. **FUS::DDIT3-mediated PDGFRB signaling leads to pericyte recruitment and sensitivity to the tyrosine kinase inhibitor imatinib in myxoid liposarcoma**
Vannas C, Tesan Tomic T, Jonasson E, Albatrok H, Andersson L, Lindén M, Grundevik P, Canfjorden V, Luna Santamaría M, Fagman H, Ståhlberg A and Åman P
Manuscript.
- IV. **Combined BRD4 and HDAC inhibition synergistically enhances anti-tumor activity in FET sarcoma models**
Vannas C, Lindén M, Jonasson E, Canfjorden V, Albatrok H, Andersson L, Ranji P, Gustafsson A, Myklebost O, Fagman H, Åman P and Ståhlberg A
Manuscript.
- V. **The levels of circulating tumor DNA and inflammatory proteins depict the clinical response in a patient with metastatic undifferentiated pleomorphic sarcoma, a case report**
Vannas C, Escobar M, Tanyasiová M, Kindeberg Sederblad M, Nyström J, Österlund T, Wennergren D, Andersson D, Dalin M, Torinsson Naluai Å, Fagman H, and Ståhlberg A
Manuscript submitted.

Additional publications, not part of this thesis:

- i. **Cell cycle and cell size dependent gene expression reveals distinct subpopulations at single-cell level**
Dolatabadi S, Candia J, Akrap N, **Vannas C**, Tomic T, Losert W, Landberg G, Åman P and Ståhlberg A
Frontiers in Genetics 2017; DOI: 10.3389/fgene.2017.00001
- ii. **FET family fusion oncoproteins target the SWI/SNF chromatin remodeling complex**
Lindén M, Thomsen C, Grundevik P, Jonasson E, Andersson D, Runnberg R, Dolatabadi S, **Vannas C**, Luna Santamaría M, Fagman H, Ståhlberg A and Åman P
EMBO Reports 2019; DOI: 10.15252/embr.201845766
- iii. **Response to BRAF/MEK Inhibition in A598-T599insV BRAF Mutated Melanoma**
Bjursten S, **Vannas C**, Filges S, Puls F, Pandita A, Fagman H, Ståhlberg A and Levin M
Case Reports in Oncology 2019; DOI: 10.1159/000504291
- iv. **Dynamic ctDNA evaluation of a patient with BRAFV600E metastatic melanoma demonstrates the utility of ctDNA for disease monitoring and tumor clonality analysis**
Vannas C, Bjursten S, Filges S, Fagman H, Ståhlberg A and Levin M
ACTA Oncologica 2020; DOI: 10.1080/0284186X.2020.1802064
- v. **FET fusion oncoproteins interact with BRD4 and SWI/SNF chromatin remodeling complex subtypes in sarcoma**
Lindén M, **Vannas C**, Österlund T, Andersson L, Osman A, Escobar M, Fagman H, Ståhlberg A and Åman P
Molecular Oncology 2022; DOI: 10.1002/1878-0261.13195
- vi. **Identification of genomic binding sites and direct target genes for the transcription factor DDIT3/CHOP**
Osman A, Lindén M, Österlund T, **Vannas C**, Andersson L, Escobar M, Ståhlberg A and Åman P
Experimental Cell Research 2023; DOI: 10.1016/j.yexcr.2022.113418

- vii. **Treatment Monitoring of a Patient with Synchronous Metastatic Angiosarcoma and Breast Cancer Using ctDNA**
Vannas C, Escobar M, Österlund T, Andersson D, Mouhanna P, Soomägi A, Molin C, Wennergren D, Fagman H and Ståhlberg A
International Journal of Molecular Sciences 2024; DOI: 10.3390/ijms25074023
- viii. **Long-Lasting Response to Lorlatinib in Patients with ALK-Driven Relapsed or Refractory Neuroblastoma Monitored with Circulating Tumor DNA Analysis**
Ek T, Ibrahim R, Vogt H, Georgantzi K, Träger C, Gaarder J, Djos A, Rahmqvist I, Mellström E, Pujol-Calderón F, Vannas C, Hansson L, Fagman H, Treis D, Fransson S, Österlund T, Chuang T, Manouk B, Ståhlberg A, Palmer R, Hallberg B, Martinsson T, Kogner P and Dalin M
Cancer Research Communications 2024; DOI: 10.1158/2767-9764.CRC-24-0338
- ix. **Deciphering the role of *FUS::DDIT3* expression and tumor microenvironment in myxoid liposarcoma development**
Ranji P, Jonasson E, Andersson L, Filges S, Luna Santamaría M, Vannas C, Dolatabadi S, Gustafsson A, Myklebost O, Håkansson J, Fagman H, Landberg G, Åman P and Ståhlberg A
Journal of Translational Medicine 2024; DOI: 10.1186/s12967-024-05211-w
- x. **Digital sequencing is improved by using structured unique molecular identifiers**
Micallef P, Luna Santamaría M, Escobar M, Andersson D, Österlund T, Mouhanna P, Filges S, Johansson G, Fagman H, Vannas C and Ståhlberg A
Genome Biology 2025; DOI: 10.1186/s13059-025-03504-x

Two Swedish popular scientific articles based on additional publications ii, iii, iv and v, originally published in “Onkologi i Sverige” are included as Appendix 1 and 2. One congress report published in “Cancerläkaren” is included as Appendix 3.

CONTENTS

Abstract	v
Sammanfattning på svenska	vii
List of papers	i
Contents.....	iv
Abbreviations	vi
1 Introduction.....	1
1.1 FET oncogene sarcomas	2
1.1.1 Myxoid liposarcoma.....	3
1.1.2 Ewing sarcoma	4
1.2 Tumor-driving mechanisms of FET fusion oncogenes	6
1.2.1 Receptor tyrosine kinase signaling.....	8
1.2.2 Heat shock protein 90.....	9
1.2.3 Angiogenesis	10
1.2.4 Epigenetics	12
1.3 Treatment monitoring of patients with sarcoma	15
2 Aims	18
3 Samples and methods.....	19
3.1 Model systems	19
3.1.1 Tumor cell lines.....	19
3.1.2 Mouse models	20
3.1.3 Human tumors and blood samples	22
3.2 Methods used for <i>in vitro</i> evaluations.....	22
3.2.1 Cell viability assays and HoloMonitor live-cell monitoring	23
3.2.2 Combination drug assays	24
3.2.3 TaqMan PCR array and quantitative PCR	26
3.2.4 RNA sequencing	27
3.2.5 Western blot	28
3.2.6 Phospho-RTK arrays.....	28

3.3	Methods used for <i>in vivo</i> evaluations	28
3.3.1	Drug treatment in PDX models	29
3.3.2	Immunofluorescence	30
3.3.3	Immunohistochemistry	30
3.4	Biomarker-based assessments and clinical evaluations	30
3.4.1	Clinical evaluations	31
3.4.2	SiMSen-Seq.....	33
3.4.3	Proximity extension assay	34
4	Results	35
4.1	Paper I	35
4.2	Paper II.....	36
4.3	Paper III.....	38
4.4	Paper IV	39
4.5	Paper V.....	41
5	Discussion	44
5.1	Model systems.....	44
5.2	Clinical applicability of drug therapies	46
5.3	Treatment monitoring.....	50
6	Conclusions	52
7	Ethical considerations	53
	Acknowledgements	54
	References	56
	Appendix	71

ABBREVIATIONS

AP	Alkaline phosphatase
BRD4	Bromodomain containing 4
CA 125	Cancer Antigen 125
CA 15-3	Cancer Antigen 15-3
CDX	Cell line-derived xenograft
cfDNA	Cell-free DNA
CRP	C-reactive protein
ctDNA	Circulating tumor DNA
Ct	Cycle threshold
CT	Computed tomography
DDIT3	DNA damage inducible transcript 3
DNA	Deoxyribonucleic acid
EWS	Ewing sarcoma
EWSR1	Ewing sarcoma breakpoint region 1
FLI1	Friend leukemia integration 1
FUS	Fused in sarcoma
GDNF	Glial cell line-derived neurotrophic factor
GEMM	Genetically engineered mouse model
GFP	Green fluorescent protein
GSEA	Gene set enrichment analysis
HDAC	Histone deacetylase
HSP90	Heat shock protein 90
IHC	Immunohistochemistry
IF	Immunofluorescence
MLS	Myxoid liposarcoma

MRI	Magnetic resonance imaging
NGS	Next-generation sequencing
PI3K	Phosphoinositide 3-kinase
PCR	Polymerase chain reaction
PDX	Patient-derived xenograft
PEA	Proximity extension assay
PET	Positron emission tomography
PRC2	Polycomb repressive complex 2
PSA	Prostate-specific antigen
RAS	Rat sarcoma virus oncogene family
RCLS	Round cell liposarcoma
RNA	Ribonucleic acid
RTK	Receptor tyrosine kinase
SDS-PAGE	Sodium dodecyl sulfate polyacrylamide gel electrophoresis
SWI/SNF	SWItch/Sucrose non-fermentable
TAF15	TATA-Box binding protein associated factor 15
TERT	Telomerase reverse transcriptase

1 INTRODUCTION

Cancer is a group of diseases characterized by uncontrolled cellular division and is the second most common cause of death globally [1, 2]. In Sweden, almost 70 000 patients were diagnosed with cancer in 2021 [3]. The most common types of cancers include prostate cancer, breast cancer, colorectal cancer and lung cancer [3]. These malignancies typically arise from epithelial cells and are referred to as carcinomas. In contrast, malignancies that arise from mesenchymal tissue, such as bones and soft tissues, are called sarcomas [4].

Sarcomas account for less than one percent of all adult cancers but represent more than 20% of all pediatric solid malignancies [4, 5]. They can be categorized into soft tissue sarcomas and bone sarcomas, with soft tissue sarcomas comprising 80-85% of cases and bone sarcomas 15-20% [6]. Sarcoma can be further divided into more than 100 histological subtypes and many more molecular subtypes, making it a heterogenous tumor family with few annual cases of each entity [7].

Cancer is generally regarded as a genomic disease, driven by mutations impacting core cellular pathways, leading to uncontrolled cellular division and growth. Typically, accumulation of multiple genomic alterations is required for the development of cancer. In sarcoma, the different entities can be categorized based on their genomic architecture, ranging from complex karyotypes with multiple chromosomal aberrations, to less complex karyotypes, driven by a few single point mutations, amplifications, or gene translocations [4, 8]. Fusion oncogene-driven sarcomas are examples of malignancies driven by a single genetic event. Fusion oncogenes arise when DNA double-strand breaks in two separate chromosomes are erroneously repaired, leading to a chromosomal translocation (Figure 1). The resulting chimeric gene may acquire oncogenic properties, potentially leading to tumor formation [9].

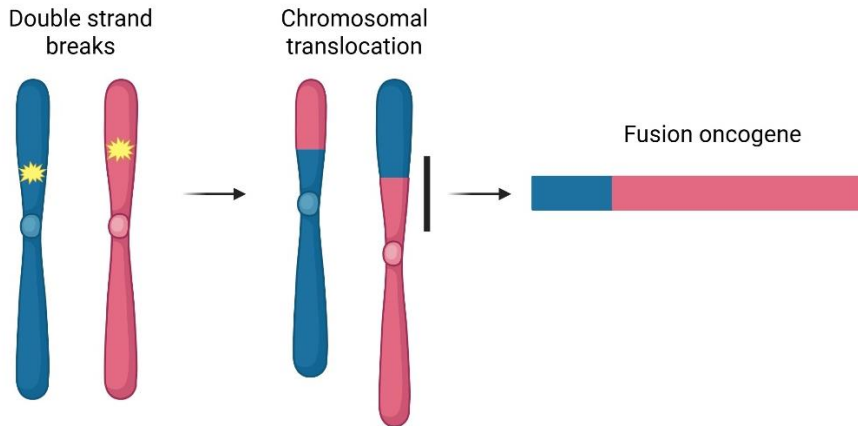


Figure 1. Model of the generation of a fusion oncogene. Fusion oncogenes can arise when DNA double-strand breaks occur on two separate chromosomes and are erroneously repaired through chromosomal translocations. This misrepair can result in the fusion of two distinct genes, potentially giving rise to a chimeric gene product with oncogenic properties. Figure created in <https://BioRender.com>.

1.1 FET ONCOGENE SARCOMAS

FET oncogene sarcomas, also known as the FET family of sarcoma, consist of malignancies driven by fusion oncogenes containing one of the FET genes *FUS*, *EWSR1* or *TAF15* as 5' partner, in combination with a transcription factor as 3' partner. *FUS*, *EWSR1* and *TAF15* are house-keeping genes, involved in RNA splicing, transportation and processing [10]. FET proteins normally interact with proteins, including other FET proteins, through their N-terminal domain, which is conserved in the fusion oncogenes. The RNA-binding domain in contrast is replaced by the DNA-binding motifs of the transcription factor partner [11, 12]. *DDIT3* and *FLI1* are the most common 3' transcription factor partners in FET fusion oncogenes. *DDIT3* is normally not expressed in cells under normal conditions, but is induced under stress, promoting cell cycle arrest and apoptosis [13]. *FLI1* is a transcription factor involved in cell differentiation, proliferation and hematopoiesis [14].

The FET family of sarcoma consists of more than ten distinct sarcoma subtypes (Figure 2) that, despite sharing similar tumor-driving mechanisms, differ significantly in their clinical presentations [15]. The two most common malignancies in the FET family of sarcoma are myxoid liposarcoma and Ewing sarcoma.

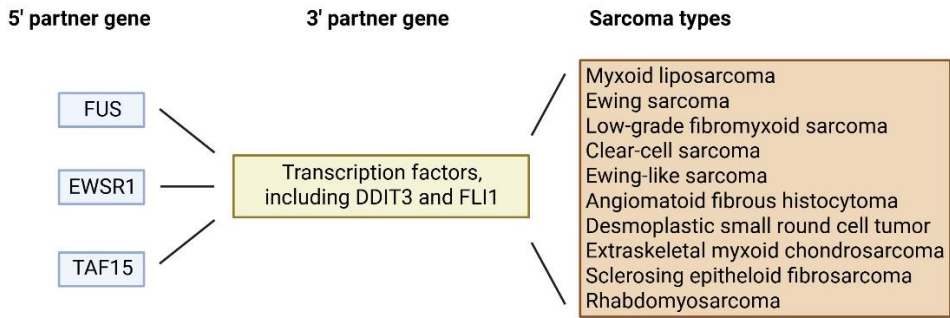


Figure 2. Sarcoma subtypes belonging to the family of FET oncogene sarcomas, with the 5' partner genes and the most common 3' partner genes of the fusion oncogenes indicated. Image adapted from [12, 16, 17].

1.1.1 MYXOID LIPOSARCOMA

Myxoid liposarcoma (MLS) is typically a slow-growing tumor that most commonly arises in the skeletal muscles of lower extremities and less frequently in the upper extremities, abdomen, thorax or neck [4, 18]. The peak incidence occurs in the fourth and fifth decade in life, although it can also affect young adults [4]. MLS is the second most common subtype of liposarcoma after well-differentiated liposarcoma [4]. The tumors are driven by specific FET fusion oncogenes, most frequently *FUS::DDIT3* or less commonly *EWSR1::DDIT3*, resulting from the chromosomal translocations $t(12;16)(q13;p11)$ and $t(12;22)(q13;q12)$, respectively [4].

MLS is histologically characterized by oval or round tumor cells embedded in a myxoid stroma, often containing mucin pools and adipoblasts (Figure 3). The tumors display a higher cellular density at the tumor periphery and a lower density centrally. A hallmark feature is the presence of thin, branching capillaries, so-called “chicken-wire” capillaries. MLS may also exhibit a more aggressive phenotype, with an increased proportion of pleomorphic round cells, sometimes referred to as round-cell liposarcoma [4]. The cell of origin for myxoid liposarcoma is believed to be a mesenchymal stem cell or progenitor cell [19, 20].

The overall prognosis is good, with a 5-year survival rate of approximately 80% [21]. Localized disease is currently treated with surgery or neoadjuvant radiation therapy, followed by surgical excision [22]. Adjuvant chemotherapy is considered if certain high-risk criteria are present, including tumor size > 8 cm, vascular invasion, tumor necrosis, infiltrative growth and/or > 5% round

cell component [23, 24]. Metastases occur in around 20% of patients, most commonly affecting other soft tissues, lungs, abdomen or bones. Approximately one in three patients with metastatic disease present with multiple metastases [25]. The 5-year survival rate for patients with metastatic disease is around 40% [26]. Treatment is typically given with chemotherapy, most commonly doxorubicin-based regimens in monotherapy or in combination therapy. Other agents that may be used include ifosfamide, gemcitabine, dacarbazine, eribulin, docetaxel and trabectedin [18].

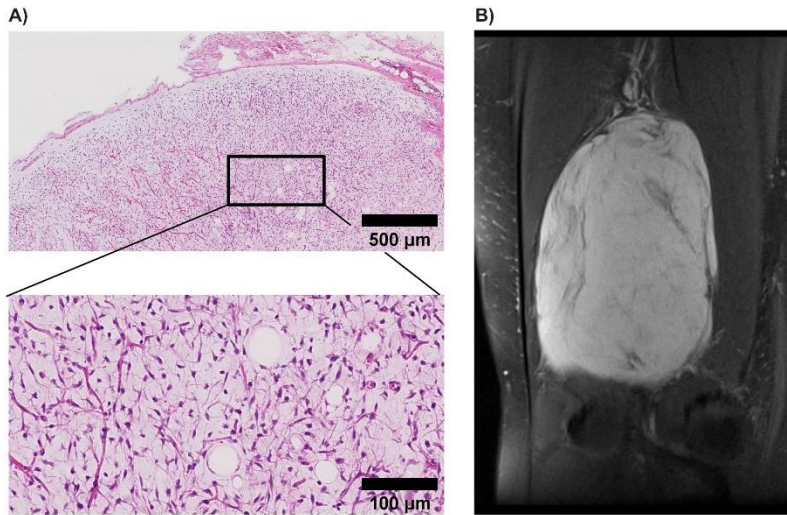


Figure 3. Histological and clinical presentation of MLS. A) Hematoxylin & Eosin staining of an MLS tumor. Lower image is an enlargement of the depicted part of the upper image. B) Magnetic resonance imaging of an MLS tumor in the right knee.

1.1.2 EWING SARCOMA

Ewing sarcoma (EWS) is the third most common bone sarcoma in adults after osteosarcoma and chondrosarcoma [27]. In the pediatric population, it ranks second after osteosarcoma [4]. The peak incidence occurs in the second decade of life with 80% of patients being below the age of 20 years. Patients above the age of 30 years are rare. EWS has a male predominance in a ratio of 1.5:1 [28]. Approximately 85% of the tumors are driven by the *EWSR1::FLI1* fusion oncogene, resulting from a $t(11;22)(q24;q12)$ chromosomal translocation. Less frequently, other fusions involving FET family genes in combination with FLI1 or related transcription factor partners occur. Recurrent secondary mutations are rare, but deletions in *STAG2*, *TP53* and *CDKN2A* are occasionally observed [29]. Chromosomal aberrations such as chromosome 1q

gain and 16q loss occasionally occur and are associated with poorer prognosis [30].

Ewing sarcoma is histologically characterized by dense groups of small, round and relatively uniform tumor cells, with the frequent occurrence of tumor necrosis (Figure 4). EWS is typically positive for the marker CD99, which in combination with fusion oncogene evaluation is used for diagnostics. However, CD99 is not specific and may also be observed in lymphomas and other soft-tissue sarcomas [31]. The precise cell of origin remains uncertain, though neural crest cells or mesenchymal stem cells are likely candidates [31, 32].

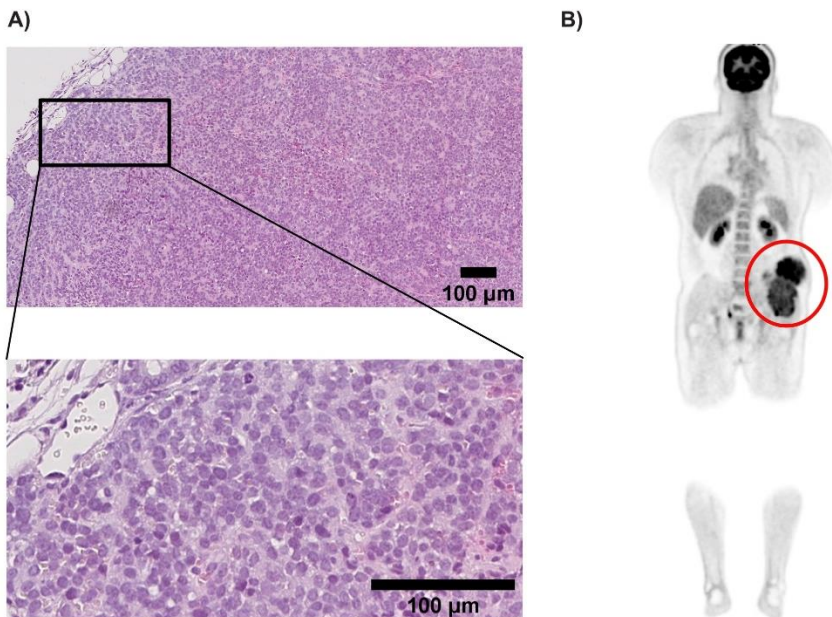


Figure 4. Histological and clinical presentation of EWS. A) Hematoxylin & Eosin staining of an EWS tumor. B) Positron emission tomography of a patient with a large EWS tumor in the left pelvis. The signals in the kidneys, bladder, liver and brain are physiological.

Clinically, EWS typically presents as a rapidly growing mass, often associated with pain and sometimes systemic inflammatory symptoms such as fever, night sweats and weight loss. It frequently arises in the diaphysis of the long bones, the pelvis or the ribs. While more than 80% of the tumors originate in bone, they can also originate from soft tissues. EWS is a highly aggressive

malignancy with a strong propensity for metastasis, most commonly to the lungs, other bones, bone marrow or soft tissues [31].

Treatment of localized disease typically involves neoadjuvant chemotherapy, surgery and/or radiation therapy, followed by additional adjuvant chemotherapy. In Sweden, the current curative treatment regimen is based on the Euro Ewing 2012 protocol, which includes 13 alternating cycles of vincristine, doxorubicin and cyclophosphamide with ifosfamide and etoposide alongside surgery and/or radiation therapy for local control [33]. Patients with metastatic disease are initially treated similarly to patients with localized disease, with curative intent if feasible. Ongoing clinical trials, including rEECur, aim to optimize treatment strategies for metastatic Ewing sarcoma [34]. The current 5-year survival rate for Ewing sarcoma is approximately 70-80% for localized disease but less than 30% for metastatic disease [35]. The intensive treatment is associated with substantial treatment-related morbidities and an elevated risk of secondary malignancies [36-38].

1.2 TUMOR-DRIVING MECHANISMS OF FET FUSION ONCOGENES

Targeting the tumor-driving fusion oncogenes seems like a logical therapeutic approach against FET oncogene sarcomas. However, no direct inhibitors of the fusion oncogenes currently exist, and the exact tumor-driving mechanism of FET fusion oncogenes remains incompletely understood. FET fusion oncoproteins have been shown to bind DNA and act as aberrant transcription factors (Figure 5A), leading to the expression of many genes involved in key cancer hallmarks such as cell-cycle regulation, cell migration, telomerase activity and growth signal transduction [39-42]. In MLS, FUS::DDIT3 not only acts as a transcription factor but also heterodimerizes with other transcription factors in the C/EBP family, thereby disrupting their normal functions such as adipogenic differentiation (Figure 5B) [43, 44]. In EWS, EWSR1::FLI1 binds to GGAA microsatellite repeats in promoters and enhancers, driving an aberrant transcriptional program [31]. The dysregulated transcriptional activity upregulates various receptor tyrosine kinases and their ligands (Figure 5C), promoting proliferative signaling pathways that may contribute to the oncogenic effects of FET fusion oncoproteins [45, 46]. Furthermore, emerging evidence suggests that FET fusion oncoproteins influence epigenetic remodeling (Figure 5D) and interact with components of the microenvironment, including the vasculature, to promote oncogenesis [31].

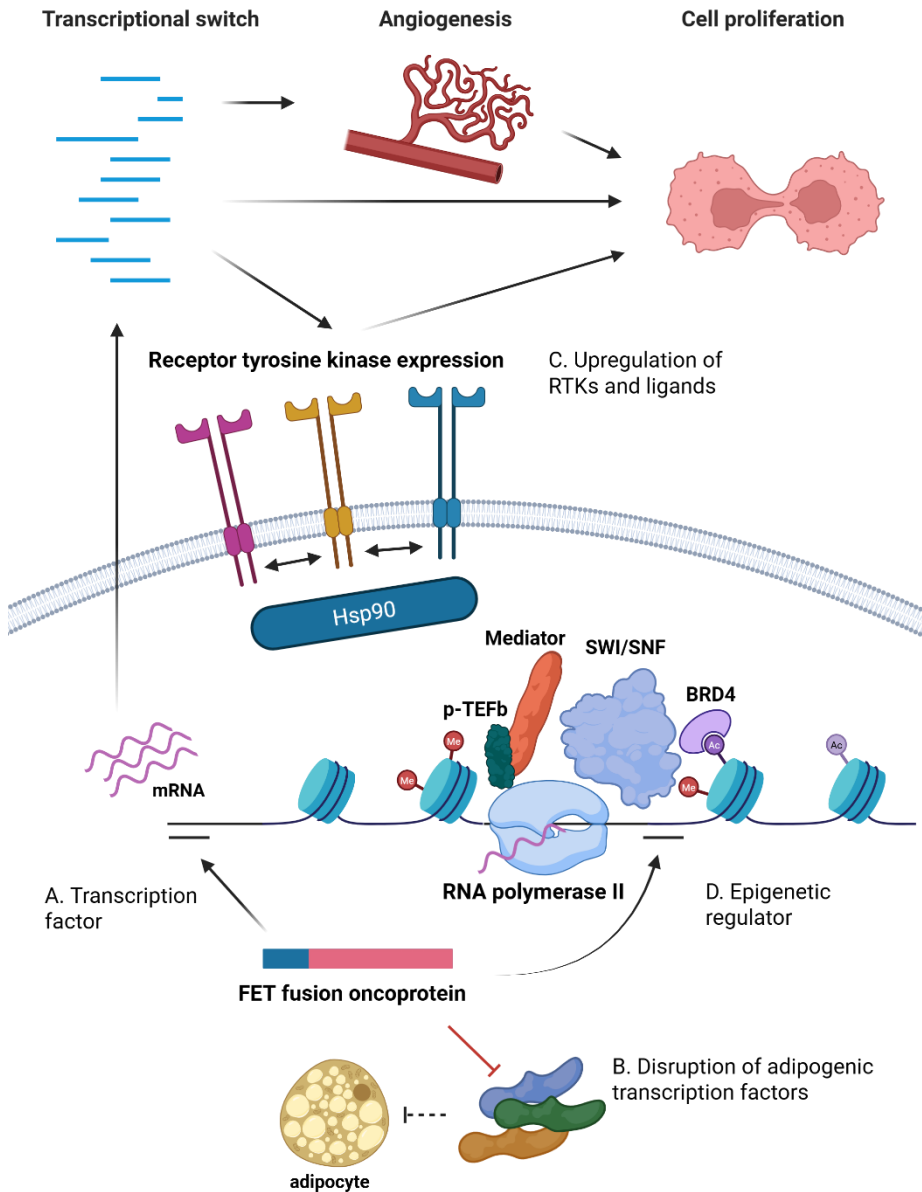


Figure 5. Model of current insights into FET fusion oncoprotein-mediated oncogenesis. FET fusion oncoproteins function as aberrant transcription factors (A), and in some cases such as in MLS, as inhibitors of transcription factors required for adipocyte differentiation (B). This leads to a transcriptional switch that promotes receptor tyrosine kinase signaling (C) and ultimately cell proliferation and angiogenesis. FET fusion oncoproteins also interact with key epigenetic regulators (D), contributing to oncogenic transcriptional reprogramming. Figure created in <https://BioRender.com>.

1.2.1 RECEPTOR TYROSINE KINASE SIGNALING

Receptor tyrosine kinases (RTKs) are transmembrane proteins that upon binding of specific ligands undergo dimerization, which activates downstream intracellular enzymatic domains. This leads to autophosphorylation of tyrosine residues and initiation of intracellular signaling cascades, ultimately regulating processes such as cell growth, proliferation and survival [47].

In MLS, overexpression of multiple RTKs including IGF1R, MET, RET, EGFR, VEGFR2 and PDGFRB has been observed [46, 48, 49]. Despite this, MLS is generally considered an RTK inhibitor-resistant malignancy. In the EORTC 62043 study, which evaluated the multi-RTK inhibitor pazopanib in metastatic soft tissue sarcomas, the liposarcoma cohort was prematurely closed due to insufficient clinical effect [50]. As a result, liposarcomas were excluded from the subsequent phase 3 PALETTE trial, which ultimately led to the approval of pazopanib for the treatment of metastatic soft tissue sarcomas [51]. To date, no RTK inhibitor is approved for use in the treatment of MLS.

In EWS, high tissue expression of IGF1R has been observed [52]. However, a clinical evaluation of the IGF1R inhibitor ganitumab did not show a significant improvement in event-free survival [53]. Overexpression of additional RTKs, such as KIT, PDGFRA, PDGFRB, EGFR and ERBB4 has also been reported in EWS tissue and cell lines [54-57]. Despite this, clinical trials investigating the multi-RTK inhibitors imatinib and regorafenib have only shown modest clinical responses [58-60]. The multi-RTK inhibitor cabozantinib has however shown more promising results in the CABONE trial, which assessed its efficacy in patients with metastatic Ewing sarcoma and osteosarcoma [61]. A clinical trial evaluating cabozantinib in combination with immunotherapy is now ongoing [62]. Furthermore, the multi-RTK inhibitor lenvatinib is being evaluated in the rEECur trial for relapsed or refractory Ewing sarcoma, but so far, no results have been published (study ID: ISRCTN36453794).

Possible explanations for the limited efficacy of RTK inhibitors in MLS and EWS include involvement of alternative oncogenic mechanisms, operating independently of RTK signaling. Additionally, resistance may be mediated by compensatory cross-activation of multiple RTKs, allowing tumor cells to bypass targeted inhibition. Many of the overactive RTKs in MLS and EWS mediate their effects through the MAPK/ERK and PI3K/AKT pathways, and resistance mechanisms in these signaling cascades may also be of importance (Figure 6). A protein that has been proposed to play a role in RTK inhibitor resistance is Heat shock protein 90 [63-66].

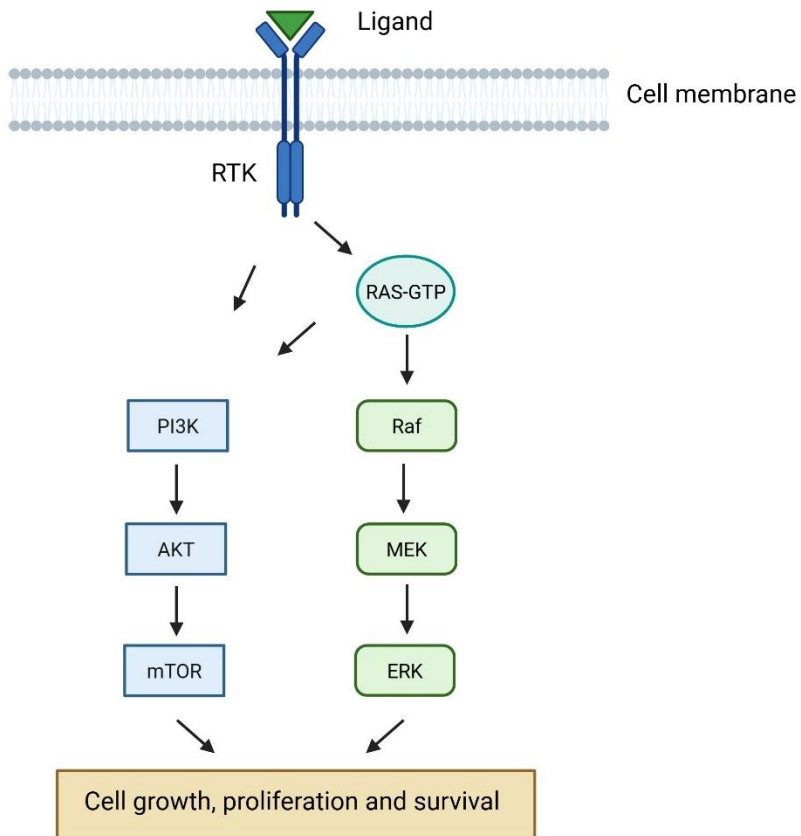


Figure 6. Principal overview of the PI3K/AKT (left) and MAPK/ERK (right) signaling pathways, two critical regulators of cell growth, proliferation, and survival in cancer. Ligand binding to RTKs initiates intracellular signaling cascades that activate these pathways. Notably, crosstalk occurs between them, as illustrated by RAS-GTP-mediated activation of PI3K [67]. Figure created in <https://BioRender.com>.

1.2.2 HEAT SHOCK PROTEIN 90

Heat shock protein 90 (HSP90) is a molecular chaperone, constituting 1-2% of the total cellular protein load under non-stress conditions [68]. Its expression is upregulated in response to stress, where it plays a critical role in the folding, stabilization, and functional maintenance of target proteins, as well as in the refolding or degradation of misfolded proteins. Several hundred proteins are known client proteins of HSP90 [69]. There are different isoforms of HSP90, with expression exclusive to the cytoplasm, endoplasmic reticulum or mitochondria. The proteins consist of an N-terminal domain that binds ATP, a middle domain involved in binding of client proteins and co-chaperones, and

a C-terminal domain mediating formation of HSP90 homodimers [70]. ATP-binding leads to a conformational change and activation of HSP90. After performing its function, ATP is hydrolyzed to ADP, leading to inactivation of HSP90 [71]. The activity of HSP90 is in turn modulated by a large group of co-chaperones [72].

In cancer, HSP90 is frequently overexpressed in both blood plasma and tumor tissues. It contributes to key cancer-related processes such as resistance to cell death, invasion/metastasis, angiogenesis and proliferation, all of which are also influenced by RTK signaling [73, 74]. Notably, many RTKs and downstream signaling proteins are HSP90 client proteins [75]. Inhibition of HSP90 has also been shown to destabilize RTKs, including members of the EGFR family and KIT, resulting in reduced signaling through the MAPK/ERK and PI3K/AKT pathways. These findings highlight the critical role of HSP90 in maintaining oncogenic signaling networks and suggest its potential involvement in mediating resistance to RTK inhibitors [63-66, 76, 77]. There are currently 22 HSP90 inhibitors in clinical trials against cancer [78]. The majority are targeting the ATP-binding N-terminal domain of HSP90, whereas a few target co-chaperone binding, the middle domain or the C-terminal domain [78]. As single agents, HSP90 inhibitors have demonstrated limited efficacy in cancer therapy. To date, pimitespib remains the only HSP90 inhibitor approved worldwide, with authorization in Japan for the treatment of advanced gastrointestinal stromal tumors (GIST) refractory to the RTK inhibitors imatinib, sunitinib, and regorafenib [79]. The drug is currently under evaluation in phase I clinical trials in the United States and Europe [80]. In MLS tissue, a high expression of HSP90 has been observed [81, 82]. Drug screenings of both MLS and EWS cell lines have identified HSP90 inhibitors as some of the most potent suppressors of cell proliferation [83, 84]. HSP90 inhibition has also been shown to reduce cell growth in EWS cell lines and mouse models resistant to IGFR1/KIT inhibitors [85], suggesting a therapeutic potential in FET oncogene sarcomas.

1.2.3 ANGIOGENESIS

Angiogenesis is the formation of new blood vessels from the pre-existing vasculature [86]. It is essential for oxygenation of tissue and is involved in normal physiological processes such as wound healing and tissue growth. Angiogenesis is tightly regulated by pro- and anti-angiogenic factors, which bind specific cell surface receptors to mediate their effect. Angiogenesis involves multiple steps, including inflammation, degradation of existing blood vessels and surrounding tissue, cell migration and formation of a primitive tube

that eventually matures and gets stabilized [86]. Our smallest blood vessels, the capillaries, consist of an inner layer of a basal membrane covered by endothelial cells and an outer layer of supporting pericytes (Figure 7). During normal angiogenesis, pro-angiogenic factors such as VEGF, angiopoietins and PDGF are secreted as a response to tissue hypoxia, binding receptors on the vascular cells, leading to proliferation and guiding of cells for formation of new blood vessels [86]. In tumors, angiogenesis is a necessity for tumor growth. In contrast to normal tissue, tumor angiogenesis is a chaotic process triggered by hypoxia, aberrant ligand secretion and upregulated receptors. Consequently, tumor capillaries are often thin, leaky and lack coverage of supporting pericytes [86]. Inhibitors of the blood vessel stimulating factor VEGF, such as bevacizumab, are used in the treatment of many malignancies [87]. However, the clinical effect has been less effective than anticipated when the drugs were introduced [88, 89].

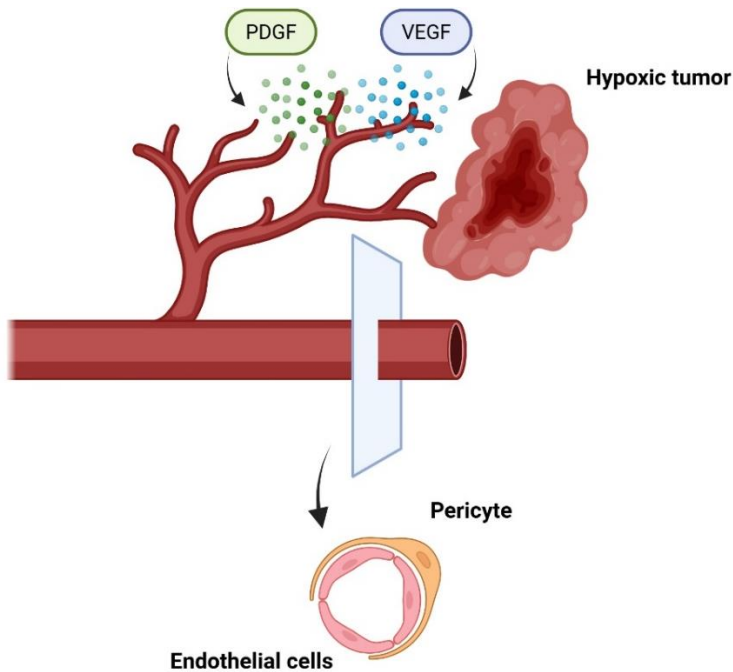


Figure 7. Simplified depiction of angiogenesis. New blood vessels sprout from existing ones in response to factors such as VEGF and PDGF, directing vessel growth toward hypoxic tissues like tumors. Below, a cross-section of a blood vessel illustrating endothelial cells (red) forming the vessel lumen, with a supporting pericyte (yellow) positioned adjacent to the vessel wall. Figure created in <https://BioRender.com>.

As mentioned in section 1.1.1, MLS exhibits a distinctive vasculature network composed of thin-walled branching capillaries, often described as “chicken-wire capillaries”. This vascular pattern serves as a diagnostic criterion, distinguishing MLS from other myxoid soft tissue tumors. However, the biological basis for this unique vascular morphology remains unknown. In contrast, EWS typically exhibits a rich vascular supply, often featuring structures known as “blood lakes”, pools of blood surrounded by CD99-positive tumor cells lacking endothelial markers [90, 91]. A high density of blood lakes has been associated with poorer patient outcomes [90]. Anti-angiogenic drugs have demonstrated only modest efficacy in MLS and EWS to date and have been investigated to a limited extent [91, 92]. Nevertheless, as RTK inhibitors also target angiogenic signaling, this strategy may hold some therapeutic potential.

1.2.4 EPIGENETICS

Another mechanism of FET fusion-driven oncogenesis is the disruption of normal epigenetic regulation. Epigenetic mechanisms modulate gene expression without altering the underlying DNA sequence. Epigenetic modifications contribute to cell type-specific gene expression and influence cellular morphology and function. Epigenetic reprogramming has also been linked to cancer, affecting many of the key processes required for tumor development [93].

The human haploid genome contains approximately three billion base pairs. DNA is tightly wrapped around proteins called histones to form condensed units known as nucleosomes. These nucleosomes are further organized into a higher-order structure called chromatin, which is tightly packed into chromosomes. Human cells are generally diploid, containing 23 pairs of chromosomes. For gene transcription to occur, chromatin must be remodeled to allow the transcriptional machinery to access the DNA. This remodeling is mediated by specific protein complexes that recognize epigenetic markers on DNA and histones, thereby modifying chromatin structure and regulating DNA accessibility (Figure 8).

Epigenetic regulation can occur at multiple levels. DNA methylation of CpG-islands in gene promoters, mediated by DNA methyltransferases, leads to gene repression. This can be reversed through demethylation, mediated by DNA demethylases [94]. Histone modifications, such as acetylation and methylation of histone tails, impact interactions between DNA and histones and consequently the packing of DNA. In principle, acetylation of histone tails,

mediated by histone acetyltransferases, results in a relaxed chromatin state and formation of transcriptionally active euchromatin. In contrast, deacetylation, mediated by histone deacetylases (HDACs) contributes to chromatin packing and formation of transcriptionally inactive heterochromatin. Methylation at various positions of histone tails can mediate both euchromatin and heterochromatin formation depending on the methylated site [95].

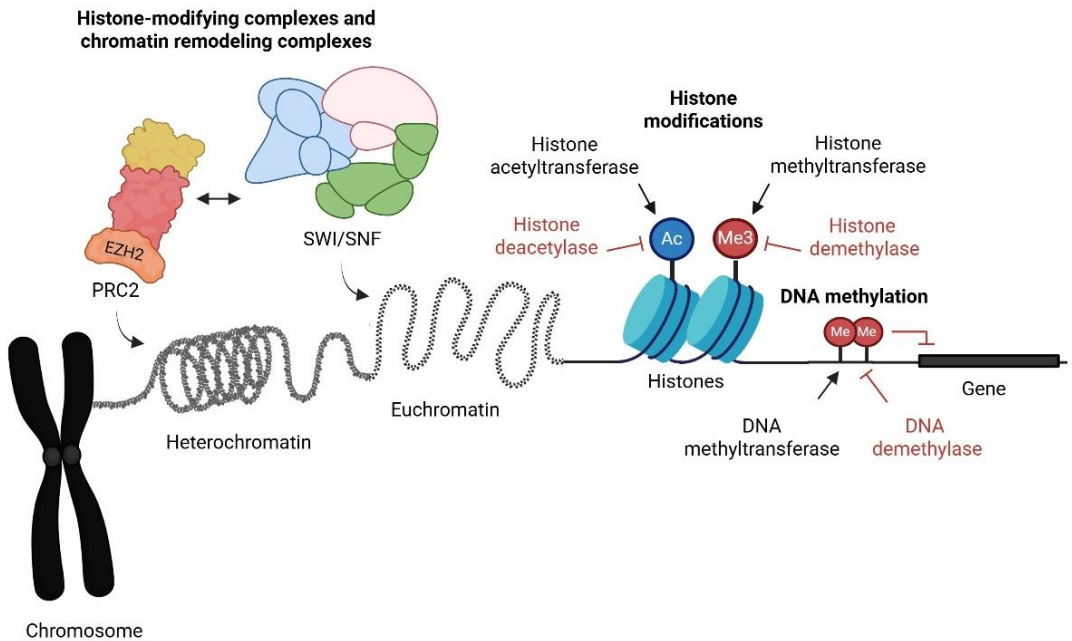


Figure 8. Summative illustration of epigenetic modifications and their mediating enzymes. Expression of genes, the protein-coding regions of DNA, is regulated by methylation of their promoter regions. DNA is wrapped around histone proteins, forming nucleosomes. Modifications to histone tails, such as methylation and acetylation, influence how tightly histones are packed. Nucleosomes further assemble into a larger structure known as chromatin. Histone-modifying complexes and chromatin remodeling complexes, including the PRC2 and SWI/SNF complexes, facilitate transitions between transcriptionally active euchromatin and transcriptionally inactive heterochromatin. Black arrows indicate stimulatory effects, while red inhibition lines indicate inhibitory effects. Figure created in <https://BioRender.com>.

The SWItch/Sucrose non-fermentable (SWI/SNF) complex is an important ATP-dependent chromatin remodeling complex that facilitates chromatin accessibility and active transcription. It consists of around 15 subunits encoded by 29 genes [96]. There are three main subtypes of SWI/SNF, often labeled as canonical BAF (cBAF), polybromo-associated BAF (PBAF) and GLTSCR1-

containing BAF (GBAF) [97]. Mutations or alterations in SWI/SNF components are found in over 20% of human cancers [96]. The SWI/SNF complex does not function by itself, but requires involvement of other chromatin remodeling complexes, histone readers and writers. An important reader is BRD4, a member of the bromodomain and extraterminal (BET) protein family [98]. BRD4 recognizes acetylated histones and accumulates at hyperacetylated sites, such as enhancer regions. The SWI/SNF complex and BRD4 interact and associate with the Mediator complex, the positive transcription elongation factor complex b (p-TEFb) and RNA polymerase II to initiate and sustain transcription [99]. In contrast, the histone-modifying Polycomb repressive complex 2 (PRC2) acts antagonistically to SWI/SNF by promoting transcriptional repression. The enzymatic subunit of PRC2, EZH2, functions as a histone methyltransferase, leading to formation of transcriptionally inactive heterochromatin [100]. Consequently, these antagonistic complexes regulate chromatin through distinct mechanisms. While the SWI/SNF complex utilizes ATP hydrolysis to remodel chromatin structure mechanically, PRC2 modifies histone tails through covalent modifications to influence chromatin conformation [101].

In addition to histone acetylation and methylation, other epigenetic modifications such as histone phosphorylation and ubiquitination, mutations in histone genes and the expression of microRNAs also influence transcriptional output in both normal cells and cancer cells [102]. These layers of regulation contribute to the complexity of epigenetic control and make the overall process challenging to fully decipher.

In FET oncogene sarcomas, FET fusion oncoproteins have been shown to accumulate at enhancer regions, characterized by histone hyperacetylation and DNA hypomethylation [103, 104]. Furthermore, their N-terminal domains interact with all three main subtypes of the SWI/SNF chromatin remodeling complex and co-localize with BRD4 on chromatin, leading to a global shift in histone methylation and disrupted transcriptional regulation [12, 104-106]. The EWSR1::FLI1 fusion oncoprotein has also been shown to promote the transcription of EZH2, the catalytic subunit of the PRC2 complex, further contributing to the imbalance in chromatin regulation [107]. Several clinical trials are currently evaluating the therapeutic potential of epigenetic drugs in FET oncogene sarcomas, including inhibitors of the histone demethylase LSD1 (ClinicalTrials.gov ID: NCT05266196) and HDACs (ClinicalTrials.gov ID: NCT04308330). However, no results have been published so far [108]. In summary, FET fusion oncoproteins drive extensive epigenetic alterations, though the precise mechanism remains incompletely understood. At present,

no epigenetic therapies are in clinical use for the treatment of FET oncogene sarcomas, although several clinical trials are ongoing.

1.3 TREATMENT MONITORING OF PATIENTS WITH SARCOMA

Patients with sarcoma are generally followed up during and after treatment through regular clinical assessments and radiological examinations, aimed at evaluating the response to therapy and detecting recurrences. Computed tomography (CT), magnetic resonance imaging (MRI) and conventional X-ray are the most frequently used imaging modalities [109]. Detecting radiological recurrences in patients with sarcoma is challenging, in particular after surgery and radiation therapy. An invasive tissue biopsy is generally necessary to confirm a disease relapse [109-111]. Moreover, CT scans and conventional X-rays expose patients to ionizing radiation, which may increase the long-term risk of radiation-induced malignancies [112]. These limitations highlight a significant unmet clinical need for improved approaches to treatment monitoring.

For many forms of cancer, blood-based tumor markers are used for disease evaluations. Some examples of tumor markers are Prostate-specific antigen (PSA) in prostate cancer, Cancer Antigen 125 (CA 125) in ovarian cancer and Cancer Antigen 15-3 (CA 15-3) in breast cancer [113]. For sarcoma, no reliable blood-based tumor marker correlating to disease status currently exists. Elevated levels of lactate dehydrogenase (LDH) are associated with poorer prognosis in soft tissue sarcoma, but the specificity is limited as LDH is elevated upon cellular lysis even in non-malignant cells [114].

Circulating tumor DNA (ctDNA) is a pan-cancer biomarker that can be detected in body fluids, such as blood, urine and saliva. The levels of ctDNA in blood plasma correlate with tumor volume and activity in most solid malignancies [115]. CtDNA consists of short DNA fragments primarily released from dying tumor cells through apoptosis or necrosis, and potentially also via active secretion in extracellular vesicles such as exosomes (Figure 9) [116]. The half-life of ctDNA in blood plasma is 15-120 minutes before being metabolized in the liver or secreted by glomerular filtration in the kidneys [115]. The amount of ctDNA in blood plasma is generally very low compared to the total amount of circulating cell-free DNA (cfDNA), excreted from healthy cells, making detection and quantification of ctDNA a challenging process. CtDNA contains tumor-related mutations that cfDNA normally lacks.

The applicability of ctDNA monitoring therefore spans from diagnostics, prognostics, treatment prediction, disease monitoring during treatment, detection of resistance mutations and evaluation of minimal residual disease, to earlier detection of recurrences [116]. Cobas EGFR Mutation Test v2, Guardant 360 CDx and FoundationOne liquid CDx are all FDA-approved ctDNA-based companion diagnostic tests used to stratify patients for targeted treatments in lung cancer [116]. Research has shown that ctDNA is a strong predictor of disease relapse and can be more sensitive and specific than radiologic evaluations for disease monitoring and relapse detection in multiple solid cancers [116]. Many techniques for ctDNA detection and quantification exist, spanning from polymerase chain reaction (PCR)-based assays, detecting a single or a few mutations with high sensitivity, to wider sequencing-based assays with next-generation sequencing (NGS), detecting multiple genetic alterations but with lower sensitivity [117]. Newer approaches of targeted sequencing using unique molecular identifiers (UMIs) have been developed for more sensitive detection of multiple genetic alterations in parallel. However, these protocols are generally complicated and time-consuming [116]. The optimal strategy for mutation detection also varies for different malignancies and mutational patterns. For malignancies with a small number of recurrent mutations, a generic panel using PCR-based assays for detection would be sufficient, covering the majority of possible genetic alterations. For patients with non-recurrent mutations, patient-specific panels using sequencing profiles from whole exome sequencing or whole genome sequencing of patients' tumors need to be generated, for subsequent monitoring either by a PCR-based assay or a targeted NGS-based method [118].

The use of ctDNA analysis for sarcoma is still in its early stages. For FET oncogenes sarcomas, a study on ctDNA quantification using digital PCR displayed a correlation between ctDNA levels and clinical outcomes in three patients with MLS [119]. Furthermore, combined mutation and translocation analysis could improve the sensitivity of ctDNA detection [120]. In EWS, detection of ctDNA at diagnosis is associated with significantly inferior survival rate [121]. Additionally, ctDNA quantification using digital PCR allows for longitudinal real-time monitoring of treatment response, but with a high inter-patient variability [122]. Other potential plasma-based markers for disease detection are epigenetic markers, metabolites or proteomic plasma profiles (Figure 9). However, their characteristics and clinical utility in remain largely unexplored [123]. In summary, disease monitoring during treatment and follow-up in patients with sarcoma is challenging. Even though many

novel approaches are under development, clinical and radiological assessments remain the gold standard in clinical routine.

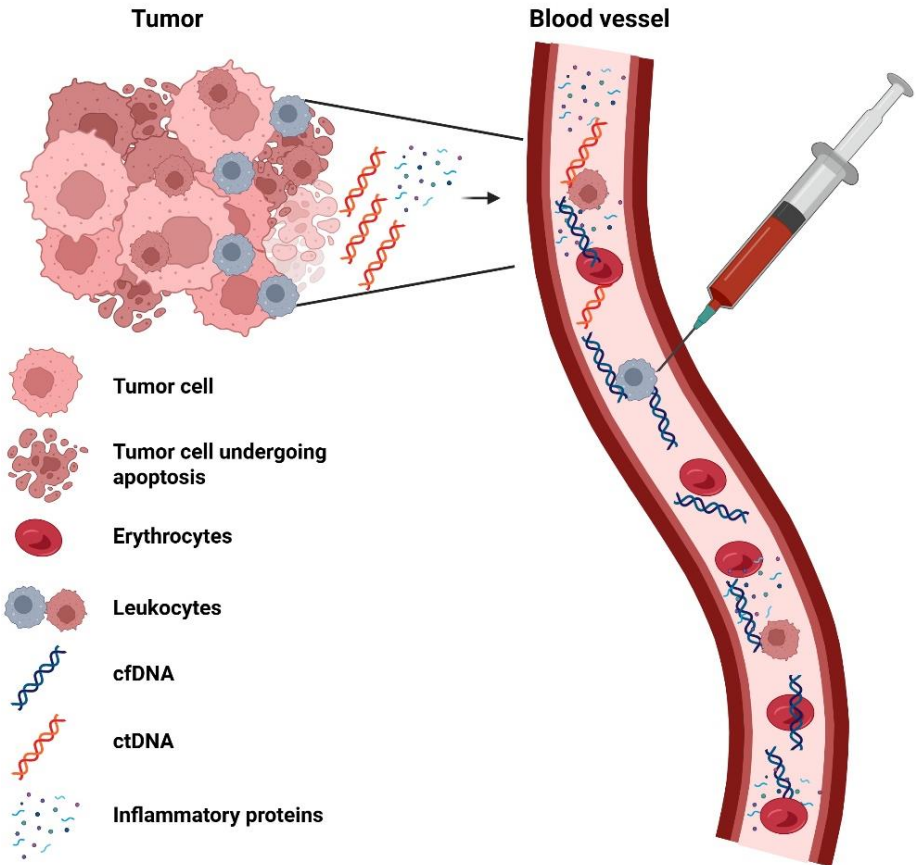


Figure 9. Overview of potential circulating biomarkers in FET fusion oncogene sarcomas. Apoptotic tumor cells release fragmented DNA, circulating tumor DNA (ctDNA), into the bloodstream. In parallel, cell-free DNA (cfDNA), derived from non-malignant apoptotic cells, is also present in circulation, generally in a much higher concentration. Inflammatory proteins are also secreted by both tumor cells and tumor-infiltrating leukocytes, further contributing to the pool of circulating biomarkers. Figure created in <https://BioRender.com>.

2 AIMS

The overall goal of this thesis was to advance therapeutic strategies and improve treatment monitoring for patients with FET oncogene sarcomas. To achieve this, we focused on identifying and evaluating targeted therapies that exploit tumor-specific molecular vulnerabilities and on developing more precise methodologies for assessing treatment response. Our approach combined *in vitro* and *in vivo* experimental models with liquid biopsy-based biomarker analyses using clinical samples. The specific aims of the papers were to:

Paper I: Investigate the therapeutic potential of HSP90 inhibition in MLS *in vitro* and *in vivo*, with a focus on overcoming resistance to targeted RET and EGFR inhibitors.

Paper II: Assess the efficacy of various HSP90 inhibitors in the treatment of MLS *in vitro* and *in vivo*.

Paper III: Characterize tumor vasculature in MLS and the factors involved in aberrant angiogenesis, to enable targeted pharmacological inhibition.

Paper IV: Assess the efficacy of epigenetic therapy using combined BRD4 and HDAC inhibition in the treatment of MLS and EWS *in vitro* and *in vivo*.

Paper V: Evaluate the utility of combined tumor-informed ctDNA monitoring and inflammatory protein profiling in blood plasma in a patient with undifferentiated pleomorphic sarcoma.

3 SAMPLES AND METHODS

This section contains a summary of the FET oncogene sarcoma experimental models and the laboratory techniques employed throughout this thesis. Further details of all the experiments performed can be found in the attached papers and manuscripts. All research was conducted with ethical approval, as detailed further in chapter 7.

3.1 MODEL SYSTEMS

The evaluation of new drugs in clinical trials is rarely initiated without strong preclinical evidence of efficacy. Consequently, experimental tumor models such as cultured tumor cell lines and mouse models are commonly used as primary tools to assess drug activity and investigate underlying mechanisms.

3.1.1 TUMOR CELL LINES

Tumor cell lines are patient-derived tumor cells that have been immortalized, either spontaneously or artificially by introduction of viral antigens, such as SV40 large T-antigen, HPV16/18 proteins E6/E7, or telomerase reverse transcriptase (TERT), to enable proliferation beyond the Hayflick limit (Figure 10) [124]. Although generating tumor cell lines can be challenging, it enables clonal expansion of tumor cells *in vitro* and supports the production of large quantities of biological material for applications such as drug screenings [125]. Tumor cell lines must be cultured under tightly controlled physical conditions, including stable temperature, humidity and CO₂ levels. Maintaining low passage numbers is also crucial to minimize the risk of secondary mutations and ensure biological consistency, thereby enhancing the reliability of the research findings. Authentication of tumor cell lines, by short tandem repeat profiling, along with regular screening for mycoplasma contamination is routinely performed to avoid experimental bias.

In this thesis, we used the MLS tumor cell lines 402-91, 1765-92 and 2645-94, that were generated by SV40 large T-antigen-mediated transformation of short-term cultured MLS tumor cells [126, 127]. Additionally, the fibrosarcoma cell line HT1080 with or without the stable transfection of a *FUS::DDIT3*-EGFP construct was used to enable comparison with the parental line and assessment of fusion oncogene-specific effects [128]. The EWS cell lines TC-71 and 6647 were derived from EWS tumor tissue and underwent

spontaneous immortalization without the need for viral transformation [129, 130].

Tumor cell lines are foundational tools in preclinical research. However, findings from tumor cell lines generally need to be validated in more biologically representative models, such as *in vivo* models or human tumor material.

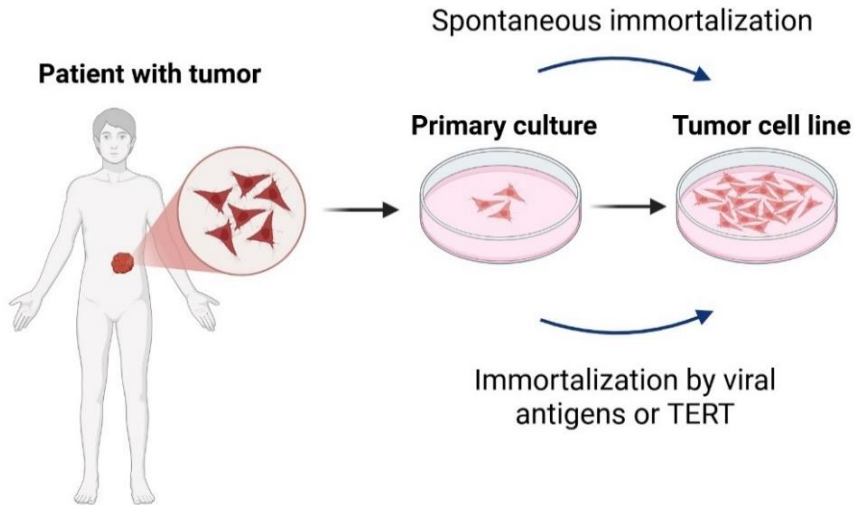


Figure 10. Generation of tumor cell lines. Tumor tissue is extracted from a patient, and the tumor cells are cultured *in vitro*. Immortalization can occur spontaneously or be induced through the introduction of viral antigens, such as SV40 or HPV proteins, or via transfection with TERT. Figure created in <https://BioRender.com>.

3.1.2 MOUSE MODELS

To validate our *in vitro* findings *in vivo*, we used both cell line-derived xenograft (CDX) and patient-derived xenograft (PDX) mouse models of MLS and EWS (Figure 11). The mice used in these studies were inbred and immunocompromised, minimizing bias from genetic variability and facilitating the engraftment of human tumors without triggering an immune rejection. Specifically, we used SCID mice, lacking both B and T lymphocytes, as well as BALB/c NUDE mice, which carry a FOXP1 gene deletion, resulting in athymia and hence T lymphocyte-deficiency [131, 132]. Despite this, BALB/c NUDE mice retain partial B lymphocyte and Natural killer-cell function. In general, SCID mice were used for establishing PDX models, whereas BALB/c NUDE mice were used for CDX models and for maintenance of fast-growing established PDX models.

Our CDX models were generated by subcutaneous injection of HT1080 fibrosarcoma cell lines, with or without stable expression of *FUS::DDIT3*, into the flanks of 4-6 weeks old female BALB/c NUDE mice. Tumor cells were suspended in fetal bovine serum and a minimum of 200 000 tumor cells were injected per mouse, to ensure tumor formation. While CDX models are relatively easy to generate, they are limited by potential genetic instability introduced during cell line immortalization. Additionally, variations between clones and laboratory conditions can reduce the reproducibility of CDX models.

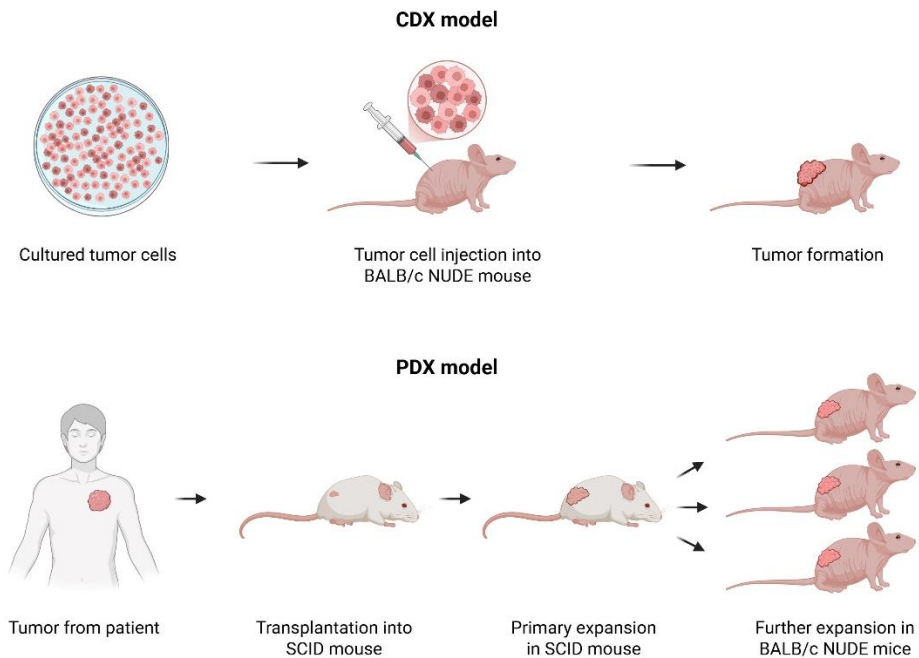


Figure 11. Mouse models used in this thesis. At the top is a CDX model, in which cultured tumor cells are injected into BALB/c NUDE mice. At the bottom is a PDX model, where a tumor obtained from a patient is transplanted into a SCID mouse. Once the tumor is established, it is further propagated by transplantation into multiple BALB/c NUDE mice to expand the model. Figure created in <https://BioRender.com>.

Our PDX models were generated from human MLS and EWS tumor tissue, generously provided by Ola Myklebost (Radiumhospitalet, Oslo). In brief, tumor fragments of approximately 2x2x2 mm were transplanted subcutaneously into the flanks of 4-6 weeks old female SCID mice for the initial engraftment. Once tumors were established, tumor pieces were serially transplanted into 4-6 weeks old female BALB/c NUDE mice for subsequent

drug treatment studies. PDX models consist of human tumors and represent the most clinically relevant *in vivo* tumor models currently available. Although they are more challenging to generate than CDX models, they retain key histological and molecular characteristics of the original tumors. However, to preserve tumor authenticity, it is critical to maintain low passage numbers, as extended passaging may result in the development of secondary mutations and alterations in tumor behavior.

3.1.3 HUMAN TUMORS AND BLOOD SAMPLES

Formalin-fixed paraffin-embedded (FFPE) human tumor samples used for immunohistochemistry were accessed through the tissue biobank at the Department of Pathology, Sahlgrenska University Hospital. In addition, we had access to blood and tumor samples from sarcoma patients enrolled in the SARKOMtest study, collected during treatment and follow-up. Blood samples from SARKOMtest participants were collected in EDTA tubes, followed by centrifugation and freezing in -80°C for long-term storage. In general, blood samples were drawn before initiation of oncological treatment, at the start of each oncological treatment modality (radiation therapy or chemotherapy cycle), before and after surgery, and at scheduled follow-up visits.

3.2 METHODS USED FOR *IN VITRO* EVALUATIONS

A range of methods was employed to evaluate drug efficacy and investigate mechanisms in treated tumor cell lines (Figure 12). This section provides a summary of the key techniques used throughout this thesis.

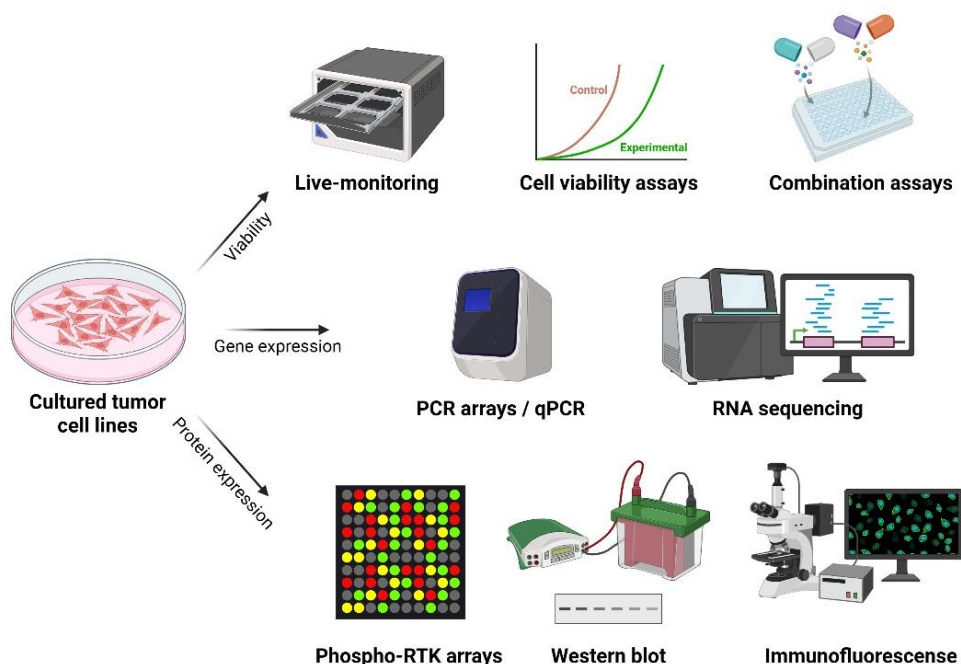


Figure 12. Summary of the experimental techniques used for *in vitro* studies in this thesis. Cultured tumor cell lines were analyzed using cell viability assays and live-cell monitoring to evaluate the treatment effects of drugs administered as monotherapy or in combination. The impact of fusion oncogene transfections and drug treatments was assessed at gene level using PCR arrays, quantitative PCR (qPCR), and RNA sequencing, and at protein level using phospho-RTK arrays, western blotting, and immunofluorescence. Figure created in <https://BioRender.com>.

3.2.1 CELL VIABILITY ASSAYS AND HOLOMONITOR LIVE-CELL MONITORING

Cell viability assays were employed to determine the cell growth-inhibiting effect of compounds on tumor cell lines. Cells were cultured in 96-well plates and treated with increasing concentrations of the tested compound. After 72 hours of drug exposure, AlamarBlue was added to evaluate metabolic viability. AlamarBlue is a blue dye that is reduced to resazurin in metabolically viable cells, leading to a color shift to pink, that can be quantified spectrophotometrically [133]. This enables calculation of IC₅₀ values, defined as the concentration required to reduce cell viability to 50% of that observed in untreated controls [134].

To enable continuous monitoring of treatment response, a HoloMonitor live-cell imaging system was used. This system employs laser-based quantitative

phase imaging to assess cell number, confluence, and volume, without the need for chemical reagents (Figure 13) [135]. By eliminating reagent use, potential biases such as toxicity or uneven loading are avoided. Additionally, the system allows for real-time monitoring of cell lines prior to extraction and subsequent RNA and protein analyses. However, these experiments are more time-consuming and require specialized holographic lids, as well as careful data interpretation and analysis to ensure reliable results. At the end of most HoloMonitor-based cell viability assays, alamarBlue was added to provide complementary data on metabolic viability.

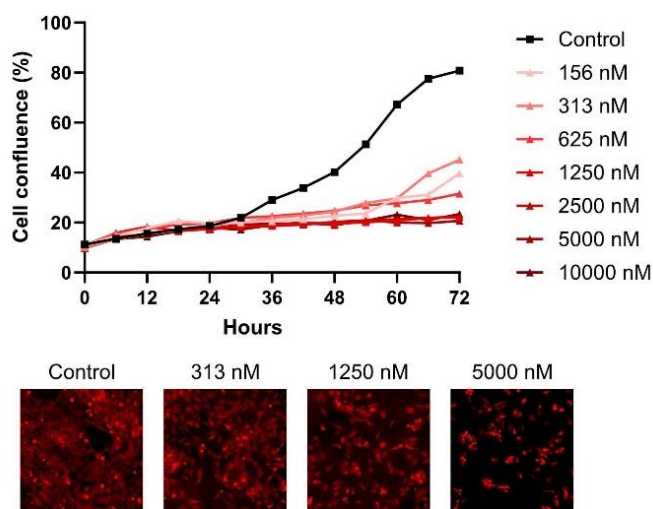


Figure 13. Example of a HoloMonitor assay tracking cell confluence every 6 hours over a 72-hour period (top). Representative images of tumor cell lines at 72 hours for the indicated drug concentrations are shown (bottom).

3.2.2 COMBINATION DRUG ASSAYS

Combination drug assays were performed in 96-well plates using a 4x4 matrix of drug combinations at varying concentrations (Figure 14). HoloMonitor assays and/or alamarBlue assays were then conducted as described above. Drug-response data were analyzed using the SynergyFinder software to evaluate potential drug synergy [136, 137]. Among the available synergy models within the software, we used the Zero Interaction Potency (ZIP) model, which offers robust performance across a wide range of concentrations, with reduced sensitivity to experimental noise [138]. Synergy was presented as a global ZIP score across the tested concentration range, where a positive ZIP score indicated synergism, a negative ZIP score antagonism whereas zero

indicated an additive drug effect (Figure 15). There is no universally accepted cutoff for defining a true synergistic effect. In large-scale drug screening studies, one or more ZIP score thresholds are sometimes applied to increase the sensitivity for detecting drug synergy [139, 140]. Another approach is to compare the ZIP score of a drug combination to that of a known synergistic combination, allowing for a comparative assessment of potential synergy [138, 139].

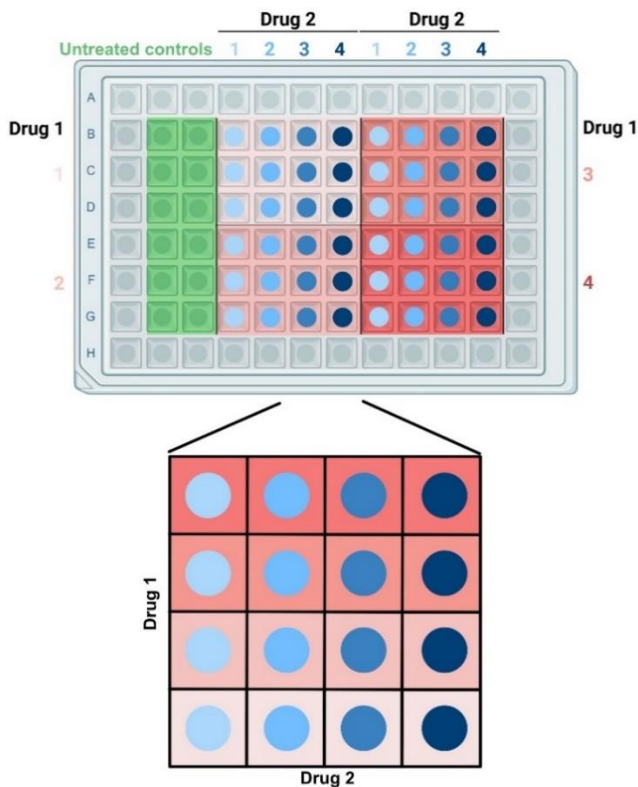


Figure 14. Example setup for a combination drug assay in 96-well plate format. The red-shaded wells represent one drug tested at increasing concentrations from low to high (1–4), while the blue dots indicate a second drug, also tested across four concentrations. Each drug combination is hence tested in triplicate, forming a 4×4 matrix as illustrated below. Peripheral wells of the 96-well plate are filled with PBS to minimize edge effects, and green-shaded wells represent untreated controls. Figure created in <https://BioRender.com>.

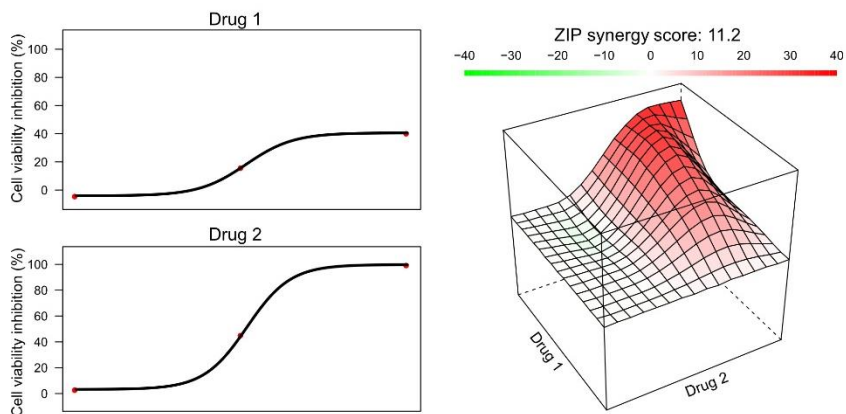


Figure 15. Example of a synergy plot using the SynergyFinder software. On the left, cell viability effect of two drugs in monotherapy. On the right, the combination effect using ZIP synergy score. Positive values (red color) indicate synergism, negative values (green color) indicate antagonism whereas zero indicates additive drug effect (white color). A global ZIP synergy score is indicated above the plot.

3.2.3 TAQMAN PCR ARRAY AND QUANTITATIVE PCR

A TaqMan PCR angiogenesis array was performed in Paper III to assess differences in gene expression between HT1080 with and without *FUS::DDIT3*. In brief, this technique uses TaqMan probes, which are short single-stranded DNA oligonucleotides that hybridize to specific target sequences located between the forward and reverse primers in individual wells. Each probe is labeled with a fluorophore at the 5' end and a quencher at the 3' end. During PCR amplification, if the target sequence is present, DNA polymerase cleaves the probe through its 5' to 3' exonuclease activity. This separates the fluorophore from the quencher, resulting in a measurable fluorescent signal. Fluorescence intensity increases with each cycle and is monitored in real time. The cycle at which the fluorescence exceeds a defined threshold is recorded as the cycle threshold (Ct) value, which is inversely proportional to the initial amount of target DNA. The Ct value reflects the starting quantity of the target gene and can be used to calculate relative gene expression levels between samples [141]. Selected genes showing differential expression in the PCR arrays were subsequently validated using SYBR-based quantitative real-time PCR with gene-specific primers and multiple biological replicates for more detailed analysis.

3.2.4 RNA SEQUENCING

RNA sequencing was employed to identify differentially expressed genes in cell lines following drug treatment. Analyses were conducted either on individual RNA-seq datasets from MLS and HT1080 cell lines (Paper III) or on grouped datasets from multiple MLS and/or EWS cell lines (Paper IV). Differentially expressed genes were analyzed using pathway enrichment analyses to identify biological pathways affected by the treatments. Gene set enrichment analysis (GSEA) was then conducted on selected gene sets to link gene expression changes to specific phenotypic traits. For example, to assess the impact of treatments on the FUS::DDIT3-driven transcriptional program, we examined gene sets containing known FUS::DDIT3 target genes that are either upregulated or downregulated. A negative normalized enrichment score for FUS::DDIT3-upregulated genes, together with a positive normalized enrichment score for FUS::DDIT3-downregulated genes, would indicate a treatment-induced reversal of the FUS::DIT3-associated transcriptional program (Figure 16).

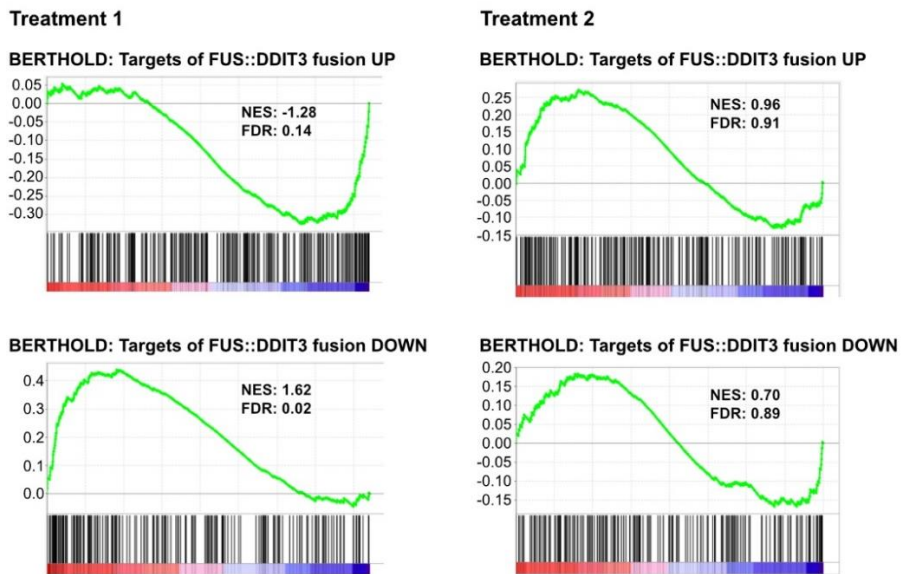


Figure 16. Gene set enrichment analyses depicting the impact of drug treatments on the FUS::DDIT3-associated transcriptional program. On the left, a drug treatment resulting in a reversal of the FUS::DDIT3-driven gene expression signature, indicated by a negative NES for FUS::DDIT3-upregulated genes and a positive NES for FUS::DDIT3-downregulated genes. On the right, a drug treatment with no significant effect on the FUS::DDIT3-mediated transcriptional output. NES; Normalized enrichment score. FDR; False-discovery rate. FDR < 0.25 was considered significant.

3.2.5 WESTERN BLOT

Western blot analysis was used for detection and quantification of target proteins following drug treatment, as described in the protocols outlined in Paper I-IV. Whole-cell protein extracts were used to enable simultaneous analysis of nuclear, cytoplasmic and pan-cellular protein expression. In brief, western blot combines protein size separation via Sodium Dodecyl Sulfate Polyacrylamide Gel Electrophoresis (SDS-PAGE) with antibody-based detection of target proteins, using specific primary and secondary antibodies. Quantification of signals was performed by normalizing the intensity of the generated bands for the proteins of interest to those of a non-regulated loading control. For drug-treated samples, results were further normalized to untreated controls to assess relative changes in protein expression. However, quantification of western blot signals should be interpreted with caution as it is susceptible to various sources of technical variability and error. The method also relies on antibody specificity and accurate estimation of protein band sizes. For target proteins that appear as multiple bands, including a positive control is essential to accurately distinguish true signal from background noise.

3.2.6 PHOSPHO-RTK ARRAYS

For large-scale screenings of drug-induced effects on phosphorylation status, phospho-RTK arrays were used. In brief, nitrocellulose membranes pre-coated with specific RTK antibodies were incubated with a protein lysate. Unbound material was washed away, and the membranes were incubated with pan-phospho-RTK secondary antibodies conjugated to horseradish peroxidase, enabling detection of phosphorylated RTKs using chemiluminescence. This method allows for a quick overview of affected RTK receptors and potentially activated signaling pathways but requires verification by western blot for more accurate quantitative assessments.

3.3 METHODS USED FOR *IN VIVO* EVALUATIONS

The effects of the fusion oncogene *FUS::DDIT3* on blood vessel constitution and signaling pathways (Paper III), as well as drug responses (Paper I-IV) were evaluated through tumor growth assessments and tissue analysis of mouse models. This section provides a summary of the key principles used to assess the *in vivo* results (Figure 17).

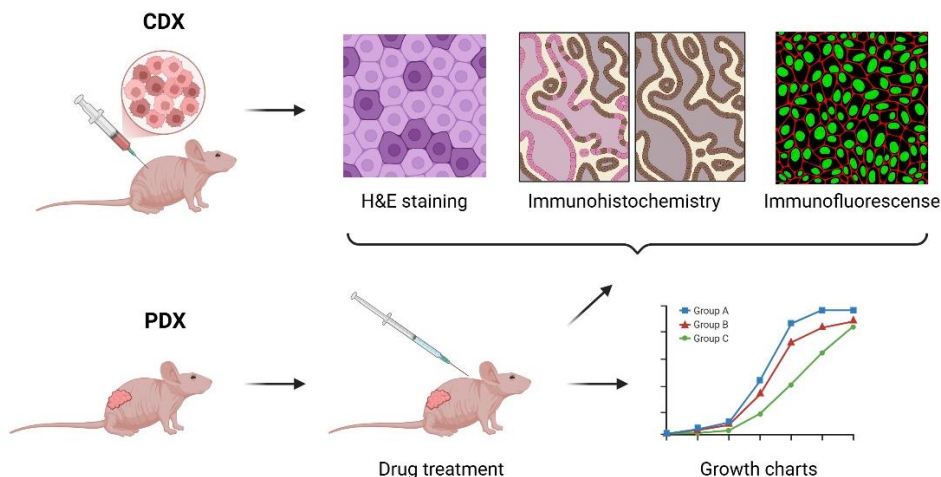


Figure 17. Summary of the experimental techniques used for our *in vivo* studies in this thesis. Above, a CDX model where injected tumor cell lines form tumors in immunodeficient mice. Below, a PDX model in which a human tumor is transplanted into immunodeficient mice. Tumors were analyzed using Hematoxylin and Eosin (H&E) staining, immunohistochemistry, and immunofluorescence. Figure created in <https://BioRender.com>.

3.3.1 DRUG TREATMENT IN PDX MODELS

Drug assessments *in vivo* (Paper I-IV) were performed on PDX mouse models. A minimum tumor size of 3x3x3 mm was required for initiation of drug studies. Therapeutic agents were administered either via intraperitoneal injection or oral gavage. Water-soluble substances were intraperitoneally injected at a maximum volume of 20 μl per gram of mouse body weight, while non-soluble compounds were administered by oral gavage in a fixed volume of 100 μl . Drugs were dissolved in DMSO and diluted in water or PBS, with Tween 20 added for oral compounds, to increase viscosity and to prevent aspiration.

During treatment, the tumor volumes of the mice were monitored by caliper, measuring the long (D) and short (d) diameter of the tumors. Tumor volumes (V) were calculated using the formula $V = \frac{\pi}{6} * D * d^2$, assuming cylindrical tumor growth. A maximum tumor volume of 2000 mm^3 was allowed and if tumors exceeded this volume, the mice were clinically evaluated and subsequently euthanized. The well-being of the mice was regularly assessed through weight monitoring and a brief clinical evaluation of behavior and mobility. Upon euthanasia, terminal blood samples were collected from all

mice prior to tumor extraction. Blood was collected in EDTA-containing Eppendorf tubes, then centrifuged and separated into plasma and cellular fractions, which were stored in separate tubes. The tumors were put in 4% formaldehyde solution for 24 hours, followed by long-term storage in 70% ethanol.

3.3.2 IMMUNOFLUORESCENCE

Visualization of target proteins in both tumor cell lines and tumor tissues was performed using immunofluorescence (IF). This technique employs fluorescently labeled primary or secondary antibodies to enable detection of multiple target proteins in parallel. It also allows for assessment of protein localization, such as restriction to specific cell types or subcellular compartments. While IF is generally not considered a quantitative method, large signal differences can be informative when the same antibodies, staining protocols and detection settings are applied across samples [142]. In paper III, IF was used to visualize protein expression in CDX and PDX tumors. All samples were processed using an identical protocol, with uniform signal thresholds being used to facilitate direct comparison between samples.

3.3.3 IMMUNOHISTOCHEMISTRY

Immunohistochemistry (IHC) was utilized in paper I-IV to visualize tissue-level expression of potential target proteins in tumor samples. Although IHC is not a quantitative method, the number of positively stained cells is often assessed manually or with an image analysis software, such as QuPath [143]. In Paper III, a double-staining IHC approach was employed to simultaneously detect two target proteins. One protein was visualized using conventional rabbit-derived primary antibodies in combination with horseradish peroxidase-conjugated secondary antibodies, producing a brown signal. The second protein was detected using primary antibodies directly conjugated to alkaline phosphatase (AP), with Fast Red serving as the chromogen, producing a red signal. This dual-staining technique allowed for comparison of protein expression and localization within the same tissue sections.

3.4 BIOMARKER-BASED ASSESSMENTS AND CLINICAL EVALUATIONS

Clinical data collection and blood sample analysis for ctDNA and inflammatory proteins were conducted in paper V. An overview of the

workflow for clinical data collection and plasma analysis is visualized in Figure 18.

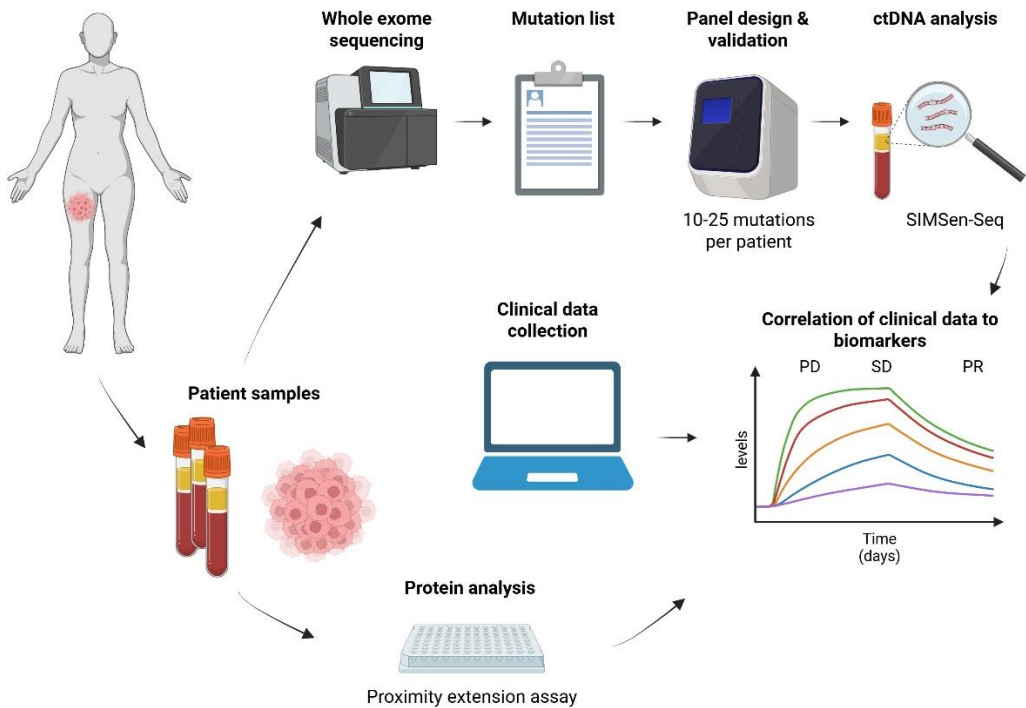


Figure 18. Overview of clinical sample collection and analyses used in this thesis. Tumor and blood samples were collected from patients and stored for downstream analysis. Tumor samples were analyzed using whole exome sequencing to generate mutation lists for subsequent ctDNA profiling of blood samples. The blood samples were also analyzed using proximity extension assays to quantify protein biomarkers. Molecular data were then integrated with clinical information for correlation analyses. Figure created in <https://BioRender.com>.

3.4.1 CLINICAL EVALUATIONS

The SARKOMtest study was initiated in 2017 at Sahlgrenska University Hospital and the University of Gothenburg, with the aim of evaluating blood-based biomarkers for monitoring treatment response in sarcoma patients. Collection of clinical data from the patients in the SARKOMtest study is continuously performed through review of the electronic medical record system Melior. Data collected includes patient diagnoses, medical history, ongoing and previous treatments, radiological evaluations and results from routine clinical blood analyses.

For the case report (paper V), radiological images were uploaded into the ARIA research software, enabling tumor contouring and volumetric analysis of individual tumor lesions and total tumor burden, an objective approach for monitoring tumor volume changes during treatment. Radiological evaluations were also retrospectively performed according to the commonly used RECIST v.1.1 criteria [144]. In brief, the RECIST criteria evaluate changes in the diameter of selected target lesions in the axial plane, across sequential radiological images (Table 1). Based on these measurements, treatment response is categorized as complete response (CR), partial response (PR), stable disease (SD) or progressive disease (PD), depending on the evolution of tumor diameters [144]. Although RECIST is routinely used in clinical studies, it has been criticized for its lack of sensitivity and specificity. Specifically, lesions that are not spherical or that grow non-horizontally may not be accurately assessed by RECIST [145].

Table 1. RECIST v1.1 criteria for radiological evaluations [144].

<p>Target lesion criteria</p> <ul style="list-style-type: none"> • Max 5 lesions in total, max 2 per organ • Lesions: ≥ 10 mm (longest axis, axial plane) • Lymph nodes: ≥ 15 mm (short axis, axial plane)
<p>Radiological evaluation</p> <ul style="list-style-type: none"> • CT (≤ 5 mm slices) or MRI • Performed ≤ 4 weeks before treatment • Same modality for all evaluations
<p>Response criteria</p> <ul style="list-style-type: none"> • Complete response (CR): All target lesions disappear • Partial response (PR): $\geq 30\%$ decrease in total lesion diameter (vs. baseline) • Progressive disease (PD): $\geq 20\%$ increase in total lesion diameter (vs. baseline or nadir), or new lesions • Stable disease (SD): Does not meet PR or PD criteria

Volumetric assessment can address these limitations by evaluating the entire tumor. However, it can be time-consuming, especially for patients with multiple lesions, since manual tumor contouring is required. Additionally, no established thresholds for defining tumor progression based on volumetric changes exist [146]. For these reasons, both volumetric assessments and RECIST evaluations were performed in Paper V. A potential bias in our retrospective RECIST evaluations is that the criteria are intended for

prospective analysis. Retrospective assessments can introduce bias, as prior knowledge of outcomes may influence the selection of tumor lesions for evaluation. To minimize this risk, we ensured that the person performing the volumetric assessment was blinded to the radiological outcomes.

3.4.2 SIMSEN-SEQ

Simple multiplexed PCR-based barcoding of DNA for ultrasensitive mutation detection by NGS (SiMSen-Seq) is a highly sensitive digital sequencing-based method, developed by Ståhlberg *et al.* in 2016 [147]. SiMSen-Seq allows for detection of mutations with low allele frequencies, suitable for analysis of ctDNA. The workflow consists of a primary PCR in which primers containing UMIs, protected by a stem-loop structure, are used to tag individual target DNA molecules (Figure 19). This is followed by a second PCR step that incorporates sequencing adapters and sample barcodes as well as amplifying the targeted products. The resulting library is purified using magnetic beads, quality control is conducted using fragment analyzer followed by sequencing using NGS. During data analysis, reads are grouped based on their UMI tags to generate consensus reads, removing PCR- and sequencing-induced errors [148]. SiMSen-Seq enables detection of mutation frequencies below 0.1%, with a rapid workflow requiring low amounts of input DNA [147].

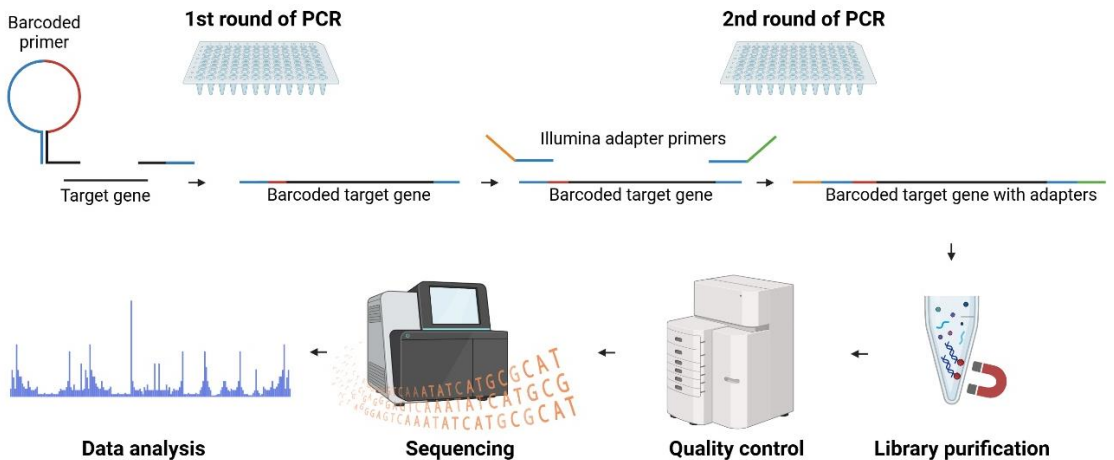


Figure 19. Summary of the SiMSen-Seq workflow. In the first round of PCR, target genes are tagged with unique molecular identifiers (UMIs, red) and adaptor sequences (blue). In the second round of PCR, the target DNA is amplified and incorporated with sequencing adapters (orange and green). The library is then purified using magnetic beads, followed by quality control using Fragment Analyzer and sequencing with NGS. The resulting data are analyzed based on UMIs to generate consensus reads. Figure created in <https://BioRender.com>.

3.4.3 PROXIMITY EXTENSION ASSAY

The relative expression of inflammatory proteins in human blood plasma samples was assessed using proximity extension assays (PEA), performed at TATAA Biocenter, Gothenburg, Sweden. This method combines antibody-based detection with PCR quantification, using pairs of antibodies labeled with DNA oligonucleotides. When two antibodies bind to the same target protein in close proximity, their attached oligonucleotides can hybridize and be extended to form a unique PCR template. Since the likelihood of antibody binding and subsequent PCR product formation correlates linearly with the amount of target protein, this method enables highly sensitive and specific detection, allowing for the calculation of relative protein levels [149]. Although PEA can currently quantify over 3,000 proteins simultaneously through newer NGS-based approaches [150], we employed a targeted panel focused on 92 inflammatory proteins, as this was the only application available at the time of analysis [151].

4 RESULTS

This is an overview of the results from respective studies, for more details see attached papers and manuscripts at the end of the thesis.

4.1 PAPER I

HSP90 inhibition blocks ERBB3 and RET phosphorylation in myxoid/round cell liposarcoma and causes massive cell death *in vitro* and *in vivo*. Oncotarget 2016.

The primary aim of this study was to identify overactive RTKs and ligands in MLS and to evaluate the efficacy of selective RTK inhibitors. We began with a meta-analysis of publicly available gene expression data from 201 human sarcoma samples, including 26 MLS tumors, which revealed that RET was more commonly expressed in MLS compared to other soft-tissue sarcomas. We confirmed the expression of RET and its ligand persephin in both cultured MLS cell lines and tumor tissues. However, treatment with the RET-specific inhibitor vandetanib failed to reduce RET phosphorylation and inhibit cell proliferation in MLS cell lines. We hypothesized that the lack of treatment response was due to cross-signaling from other RTKs, forming heterocomplexes with RET. To investigate this, we performed phospho-RTK arrays on MLS cell lines, which revealed high EGFR and ERBB3 activity. Expression of EGFR and ERBB3 was confirmed in MLS tumor tissue using IHC. Furthermore, proximity ligation assays and co-immunoprecipitation demonstrated co-localization of RET and ERBB3 in MLS cell lines, supporting the presence of heterodimeric RTK complexes. However, treatment with the EGFR inhibitor gefitinib, both as monotherapy and in combination therapy with vandetanib, showed limited efficacy in MLS cell lines with IC50 values in high micromolar concentrations.

To further explore the mechanisms driving this partial resistance, we conducted a literature search on potential protein interactions and found that RET, EGFR and ERBB3 are all client proteins of the chaperone HSP90 [152, 153]. HSP90 is involved in protein complex formation and RTK activation, making it a plausible drug target. Targeting HSP90 with the inhibitor 17-DMAG in MLS cell lines resulted in growth inhibition, with IC50 values in the low nanomolar range. Treatment with 30 nM 17-DMAG reduced the phosphorylated levels of RET and ERBB3 in MLS cell lines, indicating an inhibiting effect on RET and ERBB3 signaling. Treatment with 17-DMAG in

an MLS PDX model reduced tumor growth and induced a histological response characterized by decreased cellularity and the induction of necrosis.

These findings indicate that HSP90 facilitates the formation of auto-activating RTK complexes and may contribute to the observed resistance to specific RTK inhibitors in MLS. HSP90 inhibition with 17-DMAG effectively reduced RTK signaling *in vitro* and suppressed tumor growth in both *in vitro* and *in vivo* models, indicating its potential as a therapeutic strategy in MLS. However, 17-DMAG was discontinued shortly after this study was published, due to concerns of liver toxicity.

4.2 PAPER II

Different HSP90 Inhibitors Exert Divergent Effect on Myxoid Liposarcoma *In Vitro* and *In Vivo*. Biomedicines 2022.

Given the promising results with 17-DMAG in MLS and its subsequent discontinuation, this study aimed to evaluate whether other HSP90 inhibitors, still in clinical trials, could produce similar effects in MLS models. We reviewed currently available HSP90 inhibitors and identified 15 compounds under evaluation in clinical trials at that time [154]. From these, we selected AUY922 and STA-9090 for comparison with 17-DMAG. AUY922 was selected based on a previous study by Steinmann *et al*, demonstrating its *in vitro* efficacy against MLS cell lines, as well as its activity in a liposarcoma PDX model [82]. STA-9090 was selected based on its ongoing evaluation in multiple phase 2 clinical trials as both monotherapy and combination therapy across various malignancies, including sarcomas [154]. We found that all three HSP90 inhibitors displayed comparable efficacy in the treatment of MLS cell lines, with IC₅₀ values in the low nanomolar range. Notably, AUY922 exhibited slightly greater potency with IC₅₀ values lower than those of the chemotherapeutic agent doxorubicin, commonly used in the treatment of MLS. All compounds induced activation of cleaved caspase-3, indicating ongoing apoptosis, as well as G2/M arrest and reduced phosphorylation of the RTKs EGFR and ERBB3. Downstream signaling analysis showed that 17-DMAG and STA-9090 also reduced the activity of the MAPK and PI3K/AKT pathway proteins MEK, ERK and AKT in all MLS cell lines. In contrast, AUY922 paradoxically increased phosphorylation of MEK, ERK and AKT in the MLS cell lines 402-91 and 1765-92.

The HSP90 inhibitors were then evaluated *in vivo*, using an MLS PDX model. The selected dose of 17-DMAG was 25 mg/kg three times per week, consistent

with the dose used in paper I. The selected dose of AUY922 was 20 mg/kg three times per week, as in the previous study by Steinmann *et al* [82]. STA-9090 was initially planned at 50 mg/kg three times per week, based on previous studies [155, 156]. However, pilot testing revealed treatment-related toxicity with significant weight loss. A dose of 25 mg/kg administered twice weekly was found to be tolerable and was subsequently used for further experiments. As previously observed, 17-DMAG significantly reduced tumor growth in the MLS PDX model. STA-9090 did not lead to any tumor growth inhibition, whereas unexpectedly, AUY922-treated tumors grew faster than untreated controls. When tumors previously treated with AUY922 were re-challenged with 17-DMAG, tumor volumes decreased, indicating that resistance to HSP90 inhibitors had not developed. Histological analysis showed that AUY922-treated tumors had increased cellularity and a more aggressive phenotype, while STA-9090-treated tumors were histologically similar to untreated controls. In contrast, 17-DMAG-treated tumors exhibited reduced cellularity, consistent with previous findings in Paper I. Notably, short-term treatment with intolerable doses of STA-9090 led to a distinct morphological shift with emergence of numerous small adipoblasts, formation of vacuoles and sparse remaining tumor cells. To explore potential combination therapies, combination assays were performed in MLS cell lines, comparing the three HSP90 inhibitors with doxorubicin and trabectedin, two drugs commonly used in the treatment of MLS. All three HSP90 inhibitors displayed synergistic effects with trabectedin, but not with doxorubicin.

In conclusion, while all three evaluated HSP90 inhibitors showed similar treatment effects *in vitro*, they displayed distinct differences *in vivo*. This might be a result of insufficient dosing due to dose-limiting toxicity or the activation of downstream compensatory signaling pathways. Among the tested compounds, 17-DMAG displayed the best effect *in vivo*, while AUY922 and STA-9090 did not show any growth reduction. These findings underscore the necessity of conducting thorough PDX evaluations before proceeding to clinical trials. The combination of HSP90 inhibition with trabectedin appears promising and warrants further investigation. The combination was not validated further *in vivo* in this paper due to the risk of severe tissue necrosis associated with chemotherapeutic agents administered intraperitoneally or subcutaneously. For further evaluation, an intravenous drug administration approach would be necessary.

4.3 PAPER III

FUS::DDIT3-mediated PDGFRB signaling leads to pericyte recruitment and sensitivity to the tyrosine kinase inhibitor imatinib in myxoid liposarcoma. *Manuscript.*

The peculiar tumor vascular architecture in MLS has long remained a mystery. A prior study by our group demonstrated that transfection of the *FUS::DDIT3* fusion oncogene into the fibrosarcoma cell line HT1080 induced an MLS-like phenotype when tumors were formed in immunocompromised mice [128]. Notably, the vascular morphology closely resembled the typical MLS phenotype, indicating that *FUS::DDIT3* induces a change in vessel morphology. However, the specific secreted factors and downstream signaling pathways mediating this effect remain to be elucidated.

The aim of this study was to further investigate the mechanisms underlying the angiogenic process in MLS, with the goal of identifying pro-angiogenic factors that may serve as therapeutic targets. To explore this, we first established a dual IHC protocol that enabled simultaneous visualization of endothelial cells and supporting pericytes. We evaluated a human MLS tumor and confirmed the presence of both cell types in the tumor vasculature. Next, we evaluated the cellular composition of blood vessels in CDX models generated from HT1080 cells with or without *FUS::DDIT3* expression. We found that the vasculature of the HT1080 *FUS::DDIT3* CDX resembled the vasculature of the MLS PDX model. Furthermore, the tumors from *FUS::DDIT3*-transfected cells exhibited a lower vascular density but a significantly higher proportion of pericytes, and of endothelial cells being covered by pericytes.

To identify *FUS::DDIT3*-induced angiogenic factors, we performed a TaqMan PCR array, which revealed increased expression of the PDGFB ligand in cultured *FUS::DDIT3*-transfected HT1080 cells compared to non-transfected controls. PDGFB forms homodimers or heterodimers with PDGFA and binds the PDGFRA or PDGFRB receptors, promoting pericyte recruitment and vessel stabilization. High protein expression levels of PDGFB were confirmed in both *FUS::DDIT3*-transfected HT1080 cells and MLS cell lines, relative to placenta extract used as a positive control. Additionally, a phospho-RTK array showed elevated PDGFRB activity in MLS cell lines and in *FUS::DDIT3*-transfected HT1080 cells compared to untransfected HT1080 cells. Immunofluorescence on the *FUS::DDIT3*-transfected HT1080 CDX and the MLS PDX demonstrated high PDGFRB expression, particularly in cells staining positive for pericyte markers.

To assess the therapeutic potential of PDGFRB inhibition, MLS and HT1080 cell lines were treated with imatinib, a multi-tyrosine kinase inhibitor targeting PDGFRA, PDGFRB, ABL, KIT, and other RTKs [157]. All cell lines exhibited relative insensitivity to imatinib, with IC50 values in the 10-20 μ M range. Phospho-RTK profiling revealed only modest downregulation of PDGFRB upon imatinib-treatment. In contrast, other RTKs, such as ERBB3 and AXL were downregulated, while FGFR3 was substantially upregulated, consistent with a known resistance mechanism of imatinib [158]. RNA sequencing of treated cell lines revealed upregulation of AKT and mTOR signaling, downstream of FGFR3, further supporting the presence of an active resistance mechanism. Imatinib-treatment of an MLS PDX for four weeks resulted in a significant tumor regression. Histological analysis showed reduced tumor cell density, indicative of a partial treatment response. However, the vasculature of the imatinib-treated tumors did not show any obvious differences in vascular density, pericyte-coverage or blood vessel morphology, suggesting that imatinib did not alter the tumor vasculature.

In conclusion, our findings suggest that PDGFB-PDGFRB signaling may contribute to the unique vascular phenotype in MLS and may promote tumor growth. MLS cell lines were not sensitive to imatinib treatment *in vitro*, possibly due to upregulation of other RTKs such as FGFR3 and downstream signaling in the AKT and mTOR pathways. Treatment of the MLS PDX led to tumor regression whereas no alterations of the vasculature were observed. While imatinib treatment may provide some tumor control, it does not appear to effectively target the aberrant angiogenesis in MLS. Further studies are warranted to explore combination therapies or alternative approaches to target PDGFRB signaling and angiogenesis in MLS.

4.4 PAPER IV

Combined BRD4 and HDAC inhibition synergistically enhances anti-tumor activity in FET sarcoma models. *Manuscript.*

The aim of this study was to evaluate the therapeutic potential of epigenetic inhibitors, both as monotherapy and in combination, for the treatment of MLS and EWS. We have previously described a potential epigenetic mechanism for FET-oncogene-induced oncogenesis, involving interactions between FET fusion oncoproteins and the chromatin remodeling complex SWI/SNF [12, 105]. This interaction promotes the formation of a multi-protein transcriptional assembly involving FET fusion oncoproteins, the SWI/SNF complex, the epigenetic reader BRD4, the Mediator complex, p-TEFb and RNA polymerase

II, which induces an oncogenic transcriptional program. Another group of epigenetic regulators, HDACs are frequently aberrantly expressed in cancers. HDAC inhibitors have been shown to suppress the cell proliferation of MLS and EWS cell lines [84, 159, 160]. This prompted us to further investigate the inhibition of BRD4 and HDAC in our MLS and EWS *in vitro* and *in vivo* models.

We used the BRD4 inhibitor AZD5153, based on previous evidence of efficacy in MLS and EWS cell lines [105] and the FDA-approved HDAC inhibitor panobinostat, currently used in the treatment of multiple myeloma [161]. We found that both AZD5153 and panobinostat inhibited the cell viability of MLS and EWS cell lines, with AZD5153 showing effect in the low micromolar range and panobinostat in the low nanomolar range. Synergistic effects were observed for combined AZD5153 and panobinostat treatment in both MLS and EWS cell lines, as demonstrated by positive global ZIP scores in both alamarBlue assays and cell confluence measurements. AZD5153 in monotherapy and in combination with panobinostat led to a cell cycle shift towards G1-phase cell cycle arrest, while panobinostat and the combination treatment induced cleaved caspase-3, indicating apoptosis. AZD5153 in monotherapy induced cleaved caspase-3 in MLS, but not in EWS cell lines. Transcriptomic profiling revealed that both treatments in monotherapy and in combination led to enrichment of gene sets related to apoptosis, HDAC function, p53 signaling and hypoxia. A large portion of the differentially expressed genes overlapped between the treatments in monotherapy and combination, indicating overlapping functions. Notably, the combination treatment induced a reversal of MLS- and EWS-specific gene sets, indicating a direct disruption of FET fusion oncoprotein-driven transcriptional programs.

Treatment with AZD5153 and panobinostat in monotherapy resulted in tumor growth arrest of MLS and EWS PDX tumors. In contrast, combined AZD5153 and panobinostat treatment led to a remarkable response with significant regression of tumor volumes, along with reduced tumor cellularity and morphological features indicative of cell death. In several cases in both the MLS and EWS models, complete tumor regressions were observed, with no detectable tumor cells remaining. For many tumors, the residual tissue consisted of white and brown adipocytes of human origin, suggesting a differentiation of the tumors into benign adipose tissue. A focused reassessment of the RNA sequencing data revealed induction of genes related to brown adipogenesis. Furthermore, a downregulation of epigenetic regulators linked to early progenitor states, as well as an upregulation of epigenetic

regulators associated with differentiated cells, were observed. These findings indicate a transition from a malignant, undifferentiated phenotype to a more differentiated and benign cellular state.

In conclusion, these data reveal a promising epigenetic treatment combination, targeting the effects of FET fusion oncoprotein-driven transcriptional programs in MLS and EWS, with the potential applicability across multiple FET oncogene sarcoma subtypes. The promising preclinical effect warrants further investigation in future clinical trials.

4.5 PAPER V

The levels of circulating tumor DNA and inflammatory proteins depict the clinical response in a patient with metastatic undifferentiated pleomorphic sarcoma, a case report. *Manuscript submitted.*

There is a great need for improved methods to monitor treatment response and detect disease recurrence at an earlier stage in patients with sarcoma. At present, clinical evaluations rely on physical examinations and radiological assessments, with no validated blood-based markers available for routine monitoring. We have previously shown that ctDNA analysis using either generic or tumor-informed mutation panels can be used to monitor the treatment response in patients with melanoma and sarcoma, using the method SiMSen-Seq [162-165]. In this study, we aimed to assess the combined use of ctDNA and inflammatory protein profiling, for monitoring treatment response in a patient with metastatic high-grade undifferentiated pleomorphic sarcoma.

The patient had previously undergone surgery and adjuvant radiation therapy for a primary tumor in the right thigh. One year after completing adjuvant radiotherapy, a single lung metastasis was detected and surgically resected, followed by adjuvant chemotherapy. Another year later, the emergence of new metastases was confirmed by cytology, and palliative chemotherapy was initiated. The patient received four different treatment regimens over a span of nine months before passing away. Blood samples were collected during palliative chemotherapy when the patient participated in the SARKOMtest study. The SARKOMtest study had not yet begun when the patient received treatment for the primary tumor and the first lung metastasis, which is why no samples were collected at those times.

This case report included several novel aspects. Due to the limited tumor tissue obtained from cytological confirmation of metastatic disease, the ctDNA panel

was designed using sequencing data from the primary tumor and the first lung metastasis. The panel included as many as 23 mutations; 5 exclusive to the primary tumor, 5 exclusive to the metastasis and 13 shared between the primary tumor and the metastasis. Concurrent quantification of inflammatory proteins was performed on the blood plasma used for ctDNA analysis. Furthermore, the radiological images were analyzed volumetrically by manual tumor contouring, enabling objective assessment of both individual tumor lesions and total tumor volume, for correlation with biomarker data. We found that the total levels of ctDNA correlated well with both radiological response according to RECIST v1.1 and total tumor volume.

Over 80% of the mutations exclusive to the metastasis, as well as those shared between the primary tumor and the metastasis, were detectable in plasma during the treatment course. In contrast, none of the mutations exclusive to the primary tumor were detected, likely reflecting tumor heterogeneity and clonal selection in the metastatic setting. Including the shared mutations, over 60% of the mutations identified in the primary tumor were nonetheless detectable in blood plasma. High variant-allele frequencies in tumor tissue correlated with high variant-allele frequencies in blood plasma.

Furthermore, we identified a set of 21 inflammatory proteins showing elevated expression compared to healthy controls at the baseline sample in combination with increasing levels during disease progression. The mean plasma levels of these 21 proteins correlated well with clinical outcomes. Many of the proteins in the panel were associated with T cell recruitment or suppression. Consistent with this, IHC analysis of the tumors revealed elevated levels of CD8+ cytotoxic T cells in both the primary tumor and the lung metastasis. One of the proteins in the panel was soluble PD-L1, which is involved in T cell suppression. High levels of PD-L1 in plasma and low tissue levels of PD-L1 are also linked to poor response to immunotherapy, a treatment option currently available for this sarcoma subtype [166-170]. IHC staining of the primary tumor and the metastatic lesion confirmed that they were both PD-L1 negative. Although this patient was not treated with immunotherapy and plasma samples were collected long after the tissue samples, these findings raise a hypothetical assumption that this patient would not have benefited from immunotherapy.

In conclusion, we found that the ctDNA levels correlated to clinical parameters in this patient with undifferentiated pleomorphic sarcoma. Mutations derived from both the primary tumor and a metastatic lesion could be detected. In

contrast, mutations that were uniquely found in the primary tumor but not in the metastasis could not be detected. This is crucial information, as ctDNA panels are typically generated from primary tumors, given that biopsies of metastatic lesions can be challenging to obtain and often yield limited material. When sequencing data is available from both the primary tumor and metastatic lesions, shared mutations can be selected to maximize detection sensitivity. However, if sequencing is limited to the primary tumor, selecting multiple mutations with high variant allele frequencies is likely the best approach to optimize ctDNA detection.

Furthermore, simultaneous ctDNA quantification and proteomic profiling from the same blood samples is technically feasible and may offer additional insights into the tumor microenvironment. Additional studies are needed to validate the clinical utility of this integrated approach. Finally, our method of volumetric radiological analysis offers a more objective metric for assessing treatment response and warrants further investigation.

5 DISCUSSION

The tumor-driving fusion oncogenes in FET oncogene sarcomas have been known for over 30 years. These sarcomas are genetically stable, characterized by a low mutational burden apart from the fusion oncogenes, making them excellent model systems for studying oncogenic mechanisms. Despite extensive research, the precise mechanisms by which FET fusion oncogenes drive tumorigenesis remain incompletely understood. In this thesis, we explored targeted therapies for FET oncogene sarcomas, selecting compounds based on current understanding of FET fusion oncogene-mediated tumorigenesis. These malignancies are currently treated with conventional chemotherapies, which nonspecifically target rapidly dividing cells. While effective in many cancers, chemotherapy often causes significant side effects due to damage to healthy proliferating cells in normal tissues, such as the gastrointestinal mucosa. Moreover, it increases the risk of secondary malignancies, particularly for patients treated at a young age, which is often the case for sarcoma patients. Targeted therapies are designed to inhibit tumor-specific alterations, potentially being more effective and causing fewer off-target effects [171]. Many such therapies are now the first line treatment for metastatic disease, such as imatinib in GIST, EGFR inhibitors in EGFR-mutant lung cancer, and immune checkpoint inhibitors in melanoma [172-174]. Development of targeted therapies requires robust preclinical validation. In this work, we evaluated selected compounds in FET oncogene sarcoma models, including established tumor cell lines as well as CDX and PDX mouse models of MLS and EWS.

5.1 MODEL SYSTEMS

MLS and EWS are the two most common tumor types within the FET oncogene sarcoma family. While different FET oncogene sarcomas share similar tumor-driving mechanisms, their clinical behaviors can vary considerably, highlighting the need for further validation of our findings in additional tumor models. Due to the higher prevalence of MLS and EWS and the availability of well-established cell lines, our research primarily focused on these two entities.

While tumor cell lines remain foundational for drug research, they have limitations, one being the genetic variability of the same cell lines across laboratories, potentially affecting behaviors such as drug responses. This variability has been demonstrated in commonly used cell lines, such as HeLa

and MCF7 [175, 176]. In our studies, we used MLS and EWS cell lines, as well as an MLS-model of *FUS::DDIT3*-expressing fibrosarcoma cells, enabling direct comparison with untransfected controls to study the specific effects of the fusion oncogene. The fibrosarcoma system was used since it tolerates the introduction of the fusion oncogene without undergoing apoptosis. However, a limitation of the fibrosarcoma system is that introducing a fusion oncogene typically associated with an indolent tumor into a highly aggressive fibrosarcoma background creates a biological mismatch. As a result, the *FUS::DDIT3*-transfected cells exhibit slower growth, complicating direct comparisons with their untransfected, rapidly proliferating counterparts. A more rational approach would be to engineer tumor cell lines from the cell of origin. However, the precise cells of origin for MLS and EWS remain undefined, although mesenchymal stem cells are the most likely candidates. Studies have shown that transfection of *FUS::DDIT3* and *EWSR1:FLI1* into mesenchymal stem cells can induce tumors with transcriptional and phenotypic features similar to MLS and EWS, respectively [19, 20, 32]. Still, no stable mesenchymal stem cell-derived FET sarcoma models are currently commercially available. This underlines the importance of validating candidate drugs *in vivo*, such as in CDX and PDX systems, more precisely recapitulating the human disease.

In this thesis, we used CDX models to compare the *in vivo* effects of tumor cell lines with or without the addition of the fusion oncogene *FUS::DDIT3*. In contrast, drug response studies were conducted using PDX models established from human MLS and EWS tumors. A commonly cited limitation of both CDX and PDX models is that the tumors are typically implanted subcutaneously rather than orthotopically, at their tissue of origin [177]. However, in the case of FET oncogene sarcomas, the subcutaneous microenvironment may adequately approximate their natural context. Another major limitation of both CDX and PDX models is their reliance on immunodeficient mice, which excludes the complexity of a functional immune system in tumor formation and treatment response. Furthermore, our MLS and EWS PDX models were derived from a single human tumor each, thereby limiting the biological heterogeneity. Ideally, multiple PDX models representing a broader range of MLS and EWS tumors would have been used. However, due to the technical difficulties and the resource-intensive nature of generating such models, this was not feasible within the scope of our studies.

A more comprehensive and physiologically relevant alternative is the use of genetically engineered mouse models (GEMMs). These models are developed

in immunocompetent mice, where an inducible, site-specific recombinase system drives the expression of oncogenes and/or the deletion of tumor suppressor genes, leading to de novo tumor development [177]. Although GEMMs have been successfully developed for various sarcoma subtypes, including dedifferentiated liposarcoma, pleomorphic liposarcoma and rhabdomyosarcoma, efforts to generate GEMMs for FET oncogene sarcomas have had limited success to date [178-182]. An additional model system worth highlighting is the scaffold model. Scaffolds are derived from primary human tumors or CDX/PDX-derived tumors that are decellularized to isolate the extracellular matrix, resulting in tissue pieces that retain the structural and biochemical characteristics of the original tumor. These scaffolds can then be sectioned into multiple pieces and re-seeded with tumor cell lines, enabling the generation of multiple small tumor constructs within a three-dimensional microenvironment. One of the key advantages of scaffolds is their ability to preserve essential features of the tumor microenvironment, making them valuable for drug screening in a more physiologically relevant setting [183]. However, these models typically rely on immortalized cell lines rather than patient-derived tumor cells and do not recapitulate the complexities of *in vivo* drug treatment. Critical factors such as drug absorption, metabolism, tumor vascularization, and normal tissue toxicity are not adequately represented in this system [184]. While promising insights into tumor–microenvironment interactions in MLS have been gained using scaffold models [184], these systems cannot yet replace PDX models for comprehensive preclinical drug evaluation.

5.2 CLINICAL APPLICABILITY OF DRUG THERAPIES

Promising preclinical results do not guarantee efficacy in human patients. The complexity of human biology, including drug absorption, distribution, metabolism, toxicity, interactions with other medications and food, as well as immunological aspects, poses substantial challenges. It is estimated that only a small fraction of drugs tested preclinically advance to clinical trials, and only about 10% of drugs entering a phase 1 trial will end up as approved drugs [185]. To facilitate clinical implementation and potentially avoid phase 1 clinical trials, we focused on drugs already in clinical use or in later clinical phase trials, for our studies. Nevertheless, drug development remains unpredictable. For instance, 17-DMAG (Papers I and II) was discontinued after Paper I was published due to hepatotoxicity, whereas AZD5153 (Paper III) is no longer in clinical trials following limited efficacy in early clinical trials against hematological malignancies. Despite this, AZD5153 continues to

attract preclinical interest, particularly in sarcomas. A recent study by Chan *et al* demonstrated strong synergy between AZD5153 and the multi-RTK inhibitor Pazopanib in multiple soft-tissue sarcoma subtypes [186].

To facilitate the clinical translation of our findings, we also thoroughly investigated drug mechanisms using RNA sequencing, phospho-RTK arrays, western blot analysis and tissue analysis using IF and IHC. In this rapidly evolving era with new drug candidates, including emerging PROTAC drugs using a ubiquitin ligase for selective degradation of specific proteins [187], a deeper understanding of the drug effects can facilitate the development and application of new therapies targeting similar pathways. However, as demonstrated in Paper II, even compounds targeting the same protein can have markedly different *in vivo* effects, underscoring the necessity of *in vivo* validation before progressing to clinical trials.

The drugs evaluated in this thesis target different aspects of the FET oncoprotein-induced mechanisms presented in section 1.2 (Figure 20). Papers I and II investigated the use of HSP90 inhibitors in MLS, to overcome resistance to RTK inhibition, specifically targeting a mechanism involving RTK autoactivation. Paper III examined RTK activity and angiogenesis as downstream effects of the transcriptional program driven by FET fusion oncoproteins in MLS, including the evaluation of imatinib to suppress this aberrant signaling. Paper IV demonstrated the efficacy of combining the epigenetic drugs AZD5153 and panobinostat in the treatment of both MLS and EWS. Among the therapeutic strategies investigated, epigenetic drugs appear particularly promising, as they represent the most direct currently known strategy to inhibit the function of FET fusion oncoproteins. Epigenetic drugs have generated significant interest within the pharmaceutical industry due to their potential tumor-specific activity. Numerous agents are currently undergoing clinical evaluations across both hematological and solid malignancies [188]. Although several epigenetic drugs have been approved for hematological malignancies, their success in solid tumors remains limited. To date, Tazemetostat remains the only epigenetic drug approved by the FDA for a solid tumor, specifically for the treatment of epithelioid sarcoma [189]. Tazemetostat targets EZH2, the enzymatic subunit of the PRC2 complex. Epithelioid sarcomas frequently exhibit deletions in SMARCB1, a component of the SWI/SNF complex, leading to aberrant PRC2 activity and a corresponding vulnerability to EZH2 inhibition [190, 191]. In the context of FET oncogene sarcomas, other epigenetic drugs such as histone demethylase

inhibitors and HDAC inhibitors are currently under clinical investigation for the treatment of Ewing sarcoma [192].

In paper IV, we have shown that epigenetic drugs may act as indirect inhibitors of FET fusion oncoprotein-mediated signaling. While no drug has been definitively shown to directly target FET fusion oncoproteins, several candidates have demonstrated potential. PROTAC-based compounds for instance, have shown *in vitro* efficacy against EWS cell lines and warrant further investigation [193]. Another compound, YK-4-279, now known as TK216, was initially believed to specifically inhibit *EWSR1::FLI1* by targeting RNA helicase A, a key co-factor for the binding of *EWSR1::FLI1* to DNA/RNA and its transcriptional activity [194]. TK216 demonstrated synergistic effects with the microtubule inhibitor vincristine, and is currently being evaluated in combination with vincristine in a phase II clinical trial for relapsed Ewing sarcoma [195]. However, subsequent studies revealed that TK216 also inhibits the growth of cancer cell lines beyond Ewing sarcoma. Its mechanism of action is likely related to microtubule destabilization, albeit at a different binding site than vincristine, possibly explaining their observed synergy [196].

Trabectedin currently represents the drug with the strongest evidence for directly inhibiting FET fusion oncogene activity. Although its exact mechanism remains incompletely understood, trabectedin has been shown to disrupt the binding of FET fusion oncoproteins to DNA and to reverse transcriptional programs driven by *FUS::DDIT3* and *EWSR1::FLI1* [197-199]. While trabectedin has shown promising results in MLS, both in metastatic and neoadjuvant settings [200-203], its efficacy in Ewing sarcoma as a monotherapy has been limited [204]. To date, combination therapies involving trabectedin have not been evaluated in either MLS or EWS, although such strategies may be required to achieve meaningful clinical benefit, at least in EWS. In this thesis we evaluated the combination of HSP90 inhibitors and trabectedin, observing synergistic effects. An even more interesting approach would be combining trabectedin with dual BRD4 and HDAC inhibition. Combination therapies have demonstrated greater efficacy than monotherapies in sarcoma treatment, primarily by reducing the risk of therapeutic resistance, although this benefit may be offset by an increased risk of toxicity [205-207].

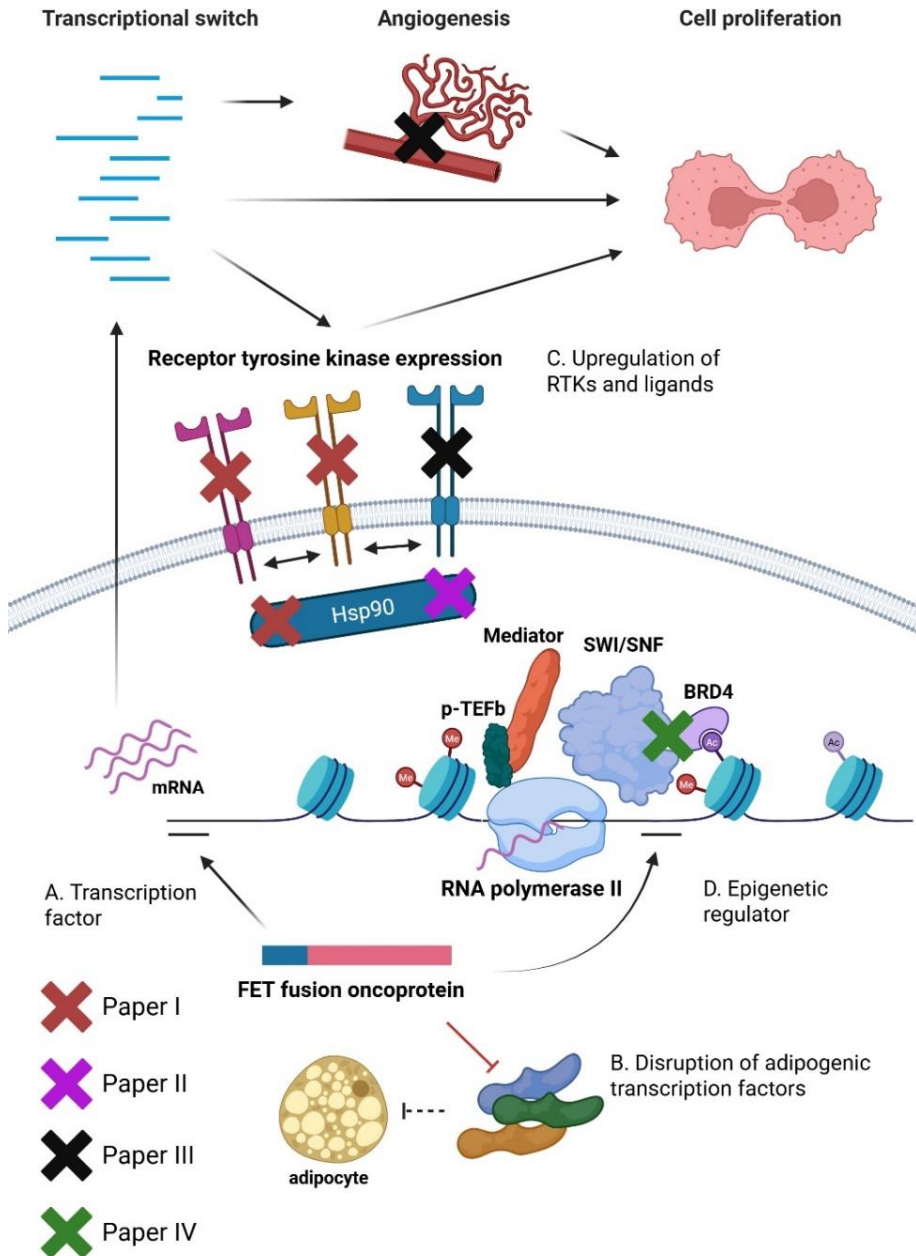


Figure 20. Schematic overview of FET fusion oncoprotein-mediated oncogenesis and the drug mechanisms evaluated across Papers I–IV. Paper I evaluated specific receptor tyrosine kinase (RTK) inhibitors. Papers I and II examined HSP90 inhibition for overcoming aberrant RTK signaling. Paper III focused on the RTK inhibitor imatinib and its potential involvement in angiogenic pathways. Paper IV investigated the use of epigenetic drugs. Figure created in <https://BioRender.com>.

In summary, this thesis aimed to evaluate potential targeted therapies for the treatment of FET oncogene sarcomas, using MLS and EWS as model tumors. We identified several targeted therapies that warrant further investigation in clinical trials. The effects of the different HSP90 inhibitors and imatinib were assessed solely in MLS, as the EWS PDX model was established after these experiments were completed. Repeating these studies in the EWS model would provide valuable insights into the relevance of these mechanisms across the broader spectrum of FET oncogene sarcomas.

5.3 TREATMENT MONITORING

In addition to identifying new therapeutic targets, this thesis explored novel strategies for monitoring treatment response using liquid biopsy. While radiological imaging remains the gold standard in routine clinical practice and clinical trials, blood-based monitoring methods such as ctDNA quantifications are increasingly being integrated into clinical trials to enable more sensitive and dynamic assessments of treatment response. Radiological assessments are typically performed at intervals of three to six months, both for patients with localized disease, after finishing treatment, for detection of disease recurrences, and for patients with metastatic disease for evaluation of treatment response. When a suspected lesion is detected, an invasive tissue biopsy is often needed to confirm a relapse before any treatment decisions are taken.

In contrast, ctDNA analysis offers an opportunity for real-time, highly sensitive and specific monitoring of cancer activity and treatment response. The negative prognostic value of detectable ctDNA in blood plasma has been demonstrated across various malignancies, both in localized disease and in metastatic settings [116]. Furthermore, the DYNAMIC study showed that postoperative ctDNA status in patients with stage II colorectal cancer could safely guide adjuvant chemotherapy decisions. After five years of follow-up, survival rates were similar between the ctDNA-guided arm and the standard arm, with fewer patients in the ctDNA-guided arm receiving chemotherapy [208]. This underscores the potential of ctDNA as a tool for tailoring treatment, potentially reducing unnecessary chemotherapy and side effects. In the context of treatment monitoring, ctDNA analysis could offer a diagnostic window where disease is detectable in blood samples but not by radiology, potentially allowing for earlier initiation of second-line treatments and improved patient outcomes. Nevertheless, it remains to be clinically validated whether ctDNA-guided monitoring translates into clinical benefit, such as increased survival [116]. Moreover, the standardization of blood sampling intervals, preanalytical

parameters, tumor material to sequence, approach, and thresholds for assessing treatment response remains an ongoing challenge [116].

The findings from Paper V offer valuable insights into the design of optimal ctDNA panels, particularly when constructed from archived tumor material. This is particularly relevant for patients monitored after treatment of localized sarcoma, where ctDNA monitoring could potentially reduce the need for some radiological examinations or help confirm relapses when imaging results are inconclusive, without the need for invasive tumor biopsies. As demonstrated in our previous case reports, ctDNA levels correlated well with clinical outcomes [162, 163, 165]. However, unlike prior studies, ctDNA analysis did not provide any lead time over radiological evaluations, likely due to the extended intervals between blood sample collections in this patient.

Additionally, paper V highlights the promise of multi-omic analyses. However, it did not clarify whether plasma protein panels reflect changes within the tumor microenvironment or represent a systemic response to the tumor and its treatment. A study by Huang *et al* in colorectal cancer demonstrated that plasma levels of cytokines such as IL-6 and IFN- γ correlated with tumor infiltration by CD8⁺ T cells and immunosuppressive M2 macrophages. Interestingly, elevated plasma levels of IL-6 were paradoxically associated with improved prognosis [209]. In contrast, for sarcoma patients, elevated serum levels of IL-6 and C-reactive protein (CRP) are associated with worse survival outcomes. To our knowledge, no study in sarcoma has investigated the relationship between inflammatory proteins in blood plasma and the tumor infiltration of immune cells. It is important to note that our findings are based on a single case report and should therefore be interpreted with caution when considering broader applications. Further studies are necessary to evaluate the interplay between inflammatory proteins, clinical outcomes, and potential treatment prediction in sarcoma.

6 CONCLUSIONS

We have explored potential therapeutic strategies targeting FET fusion oncogene-specific mechanisms, employing both *in vitro* and *in vivo* models. By using MLS and EWS as representative FET oncogene sarcomas, we have assessed a range of distinct pharmacological inhibitors with potential applicability for multiple members within this tumor family. The findings provide a rationale for advancing these therapies into clinical trials, where treatment monitoring using tumor-informed ctDNA analysis could serve as a tool for improved evaluation of clinical response.

Paper I: We showed that inhibition of HSP90 using the compound 17-DMAG can reduce RTK signaling in MLS cell lines resistant to targeted EGFR and RET RTK inhibitors, leading to cell death both *in vitro* and *in vivo*.

Paper II: We demonstrated that three different HSP90 inhibitors led to similar *in vitro* responses, while their efficacy in MLS PDX models varied significantly. This study emphasizes the importance of careful evaluation of drugs with similar molecular targets in PDX models before advancing to clinical trials in humans.

Paper III: We demonstrated that *FUS::DDIT3* expression altered the tumor vasculature in MLS CDX and PDX models, with increased pericyte coverage, potentially through PDGFB-mediated activation of PDGFRB. Treatment with the multi-RTK inhibitor imatinib reduced tumor growth in the MLS PDX model but did not alter vascular morphology.

Paper IV: We showed that combined epigenetic inhibition targeting BRD4 and HDACs is very effective in both MLS and EWS experimental models. The treatments reversed the FET fusion oncoprotein-induced gene expression profiles and induced brown adipogenesis and apoptosis.

Paper V: We showed that tumor-informed ctDNA analysis combined with profiling of inflammatory proteins could be used to monitor the treatment response in a patient with metastatic high-grade sarcoma, providing additional information relevant for clinical treatment decisions.

Overall, this thesis offers a meaningful contribution to the expanding body of research aimed at improving therapeutic outcomes for patients with FET oncogene sarcomas.

7 ETHICAL CONSIDERATIONS

All animal experiments were conducted in accordance with the EU directive 2010/63 with ethical approval issued by regional animal ethics committee of Gothenburg DNR 277-2012, date of approval 2012-10-19; DNR 129-2016, date of approval 2016-12-14; DNR 23035-2021, date of approval 2022-01-26 and regional ethical committee South-Eastern Norway DNR 2020/1244/REK sør-øst, date of approval 2016-11-16. We adhered to the principles of 3Rs (Replacement, Reduction and Refinement) to the greatest extent possible, minimizing the number of animals used and reusing tumor and healthy tissue across projects when feasible. Performing animal experiments to evaluate drug effects *in vivo* is currently a necessity to proceed into human clinical trials as no equivalent alternative exists. The medical benefit of our research therefore outweighs the risks.

Human tumor samples for immunohistochemistry analysis were obtained from the tissue bank at the Department of Pathology, Sahlgrenska University Hospital. Ethical approval for retrieval and analysis of samples was granted by the regional ethical review board in Gothenburg, DNR 133-11, date of approval 2011-04-18.

The collection of blood samples, tumor tissue and clinical data from patients enrolled in the SARKOMtest study was approved by the regional ethical review board in Gothenburg DNR 485-16, date of approval 2016-06-23 with amendments T-795-16, date of approval 2016-09-15; T525-18, date of approval 2018-06-15; and 2021-04895, date of approval 2021-10-24. Blood samples of healthy individuals were obtained from the PREAN study, was approved by the regional ethical review board in Gothenburg DNR 054-15, date of approval 2015-05-18. The collection of samples posed minimal risk to the patients. All participants provided written informed consent, and no payment or other compensation was offered for participating in the studies.

ACKNOWLEDGEMENTS

This work is dedicated to patients with sarcomas and their families and friends, with the hope of contributing to a deeper understanding of these diseases, better outcomes, and improved quality of life. I extend my deepest gratitude to all the patients who participated in our studies, generously providing samples and sharing their time to help advance healthcare for others.

To my supervisor, **Pierre Åman**, one of the kindest individuals I know, with an extraordinary breadth of scientific knowledge and curiosity. I am truly sorry for having delayed your well-deserved retirement for so many years.

To my co-supervisor, **Anders Ståhlberg**, among the brightest and most driven researchers I have had the privilege to work with. You have consistently been my greatest support during the moments I needed it the most.

To my co-supervisor and clinical mentor, **Max Levin**, a true inspiration. Your remarkable clinical expertise, combined with deep scientific insight, has left a lasting impression on me.

To my co-supervisor, **Göran Landberg**, thank you for your steady support and invaluable guidance during critical moments in my career.

To **Henrik Fagman**, one of the sharpest and funniest people I know. This work simply would not have been possible without your insight, support, and encouragement. Though not formally listed, I consider you both a co-supervisor and a mentor, and I am deeply grateful for everything you have contributed.

To all my current and former colleagues at the **Sahlgrenska Cancer Center** and the **Oncology Clinic**, thank you for your support, encouragement, and laughter throughout this journey. **Ella** and **Karolina**, thank you for kindly agreeing to be toastmasters at my dissertation party, despite being in the final stretch of your own dissertations.

To my original research group: **Malin, Emma, Soheila, Pernilla, and Mandy**. You were the foundation that made this work possible, and your collaboration, support, and dedication have been invaluable.

To my extended research family: **Daniel, Anna, Tobias, Parmida, Lisa, Manuel, Firaol, Pia, Vilma, Mathilda** and **Julia**. Your support has been immeasurable, and I am forever grateful for all the help you have given me, far more than I could ever repay.

To my closest clinical colleagues on the sarcoma team: **Lina Hansson, Petra Wieveg, Marie-Louise Larsson, Karolina Pontén** and **Claes Molin**. Thank you for your constant support, guidance, and collaboration every day. Your contributions have been invaluable.

To my extended clinical partners at the **Tumor Orthopedics Department, Radiology Department,** and **Pathology Department**. Together, we form an incredible team, and I am deeply grateful for your expertise and collaboration.

To **Biobank Väst**, for your invaluable assistance and expertise in blood samples and tissue sample collection and storage.

To my dear friend and research nurse, **Christina Turesson**, your friendship and unwavering dedication have meant more to me than words can express. You and **Vivika** are truly the best research nurses anyone could wish for.

To my friends, in particular **Viktor, Daniel, Oscar, Rickard, Ado, Jonas, Simon, Bea** and **Kasia**. Thank you for your unwavering support, loyalty, and encouragement throughout this journey.

To my **close and extended family**, I am eternally grateful to have you all around me. Most of all, to my beloved **Kahina** and **Oscar**, *Tout ce que je fais, c'est l'écho de mon amour pour vous.* To our deeply missed **baby angel boy**, *tu vis dans nos cœurs.*

Finally, I am profoundly grateful to our sponsors and grant providers; Johan Jansson foundation, Assar Gabrielsson foundation, Swedish Childhood Cancer Foundation, Swedish Cancer Society, Anna-Lisa and Bror Björnsson Foundation, the sarcoma patient union research fund, the memorial fund of Elvira Trané, Lions Cancer Fund West, Sahlgrenska University Hospital funds, The Gothenburg Society of Medicine, Sweden's Innovation Agency, the Sjöberg Foundation, Region Västra Götaland and the Swedish state under the agreement between the Swedish government and the county councils, the ALF-agreement. Without your generous support, none of this would have been possible.

REFERENCES

1. Collaboration, G.B.o.D.C., *Cancer Incidence, Mortality, Years of Life Lost, Years Lived With Disability, and Disability-Adjusted Life Years for 29 Cancer Groups From 2010 to 2019: A Systematic Analysis for the Global Burden of Disease Study 2019*. *JAMA Oncology*, 2022. **8**(3): p. 420-444.
2. Hanahan, D. and R.A. Weinberg, *The hallmarks of cancer*. *Cell*, 2000. **100**(1): p. 57-70.
3. Socialstyrelsen, c., *Cancer i siffror*. 2023.
4. Fletcher, C., D.M., *Pathology and Genetics of Tumours of Soft Tissue and Bone*. World Health Organization Classification of Tumours, 2002.
5. Burningham, Z., et al., *The Epidemiology of Sarcoma*. *Clinical Sarcoma Research*, 2012. **2**(1): p. 14.
6. Stiller, C.A., et al., *Descriptive epidemiology of sarcomas in Europe: Report from the RARECARE project*. *European Journal of Cancer*, 2013. **49**(3): p. 684-695.
7. Sbaraglia, M., E. Bellan, and A.P. Dei Tos, *The 2020 WHO Classification of Soft Tissue Tumours: news and perspectives*. *Pathologica*, 2021. **113**(2): p. 70-84.
8. Taylor, B.S., et al., *Advances in sarcoma genomics and new therapeutic targets*. *Nature Reviews Cancer*, 2011. **11**(8): p. 541-557.
9. Hahn, Y., et al., *Finding fusion genes resulting from chromosome rearrangement by analyzing the expressed sequence databases*. *Proc Natl Acad Sci U S A*, 2004. **101**(36): p. 13257-61.
10. Schwartz, J.C., T.R. Cech, and R.R. Parker, *Biochemical Properties and Biological Functions of FET Proteins*. *Annu Rev Biochem*, 2015. **84**: p. 355-79.
11. Thomsen, C., et al., *A conserved N-terminal motif is required for complex formation between FUS, EWSR1, TAF15 and their oncogenic fusion proteins*. *Faseb j*, 2013. **27**(12): p. 4965-74.
12. Linden, M., et al., *FET family fusion oncoproteins target the SWI/SNF chromatin remodeling complex*. *EMBO Rep*, 2019. **20**(5).
13. Jauhiainen, A., et al., *Distinct cytoplasmic and nuclear functions of the stress induced protein DDIT3/CHOP/GADD153*. 2012. **7**(4): p. e33208.
14. Truong, A.H.L. and Y. Ben-David, *The role of Fli-1 in normal cell function and malignant transformation*. *Oncogene*, 2000. **19**(55): p. 6482-6489.
15. Aman, P. *Fusion genes in solid tumors*. in *Seminars in cancer biology*. 1999. Elsevier.

16. Schöpf, J., et al., *Multi-omic and functional analysis for classification and treatment of sarcomas with FUS-TFCP2 or EWSR1-TFCP2 fusions*. Nature Communications, 2024. **15**(1): p. 51.
17. Warmke, L.M. and J.M. Meis, *Sclerosing Epithelioid Fibrosarcoma: A Distinct Sarcoma With Aggressive Features*. 2021. **45**(3): p. 317-328.
18. Abaricia, S. and A.C. Hirbe, *Diagnosis and Treatment of Myxoid Liposarcomas: Histology Matters*. Curr Treat Options Oncol, 2018. **19**(12): p. 64.
19. Riggi, N., et al., *Expression of the FUS-CHOP Fusion Protein in Primary Mesenchymal Progenitor Cells Gives Rise to a Model of Myxoid Liposarcoma*. Cancer Research, 2006. **66**(14): p. 7016-7023.
20. Rodriguez, R., et al., *Expression of FUS-CHOP fusion protein in immortalized/transformed human mesenchymal stem cells drives mixoid liposarcoma formation*. Stem Cells, 2013. **31**(10): p. 2061-72.
21. Zhao, J., et al., *Survival and prognostic factors among different types of liposarcomas based on SEER database*. Scientific Reports, 2025. **15**(1): p. 1790.
22. Lansu, J., et al., *Dose Reduction of Preoperative Radiotherapy in Myxoid Liposarcoma: A Nonrandomized Controlled Trial*. JAMA Oncol, 2021. **7**(1): p. e205865.
23. Sundby Hall, K., et al., *Adjuvant chemotherapy and postoperative radiotherapy in high-risk soft tissue sarcoma patients defined by biological risk factors-A Scandinavian Sarcoma Group study (SSG XX)*. Eur J Cancer, 2018. **99**: p. 78-85.
24. Haniball, J., et al., *Prognostic Factors and Metastatic Patterns in Primary Myxoid/Round-Cell Liposarcoma*. 2011. **2011**(1): p. 538085.
25. Moreau, L.-C., et al., *Myxoid/Round Cell Liposarcoma (MRCLS) Revisited: An Analysis of 418 Primarily Managed Cases*. Annals of Surgical Oncology, 2012. **19**(4): p. 1081-1088.
26. Shinoda, Y., et al., *Prognostic factors of metastatic myxoid liposarcoma*. BMC Cancer, 2020. **20**(1): p. 883.
27. Dorfman, H.D. and B. Czerniak, *Bone cancers*. Cancer, 1995. **75**(1 Suppl): p. 203-10.
28. Jawad, M.U., et al., *Ewing sarcoma demonstrates racial disparities in incidence-related and sex-related differences in outcome: an analysis of 1631 cases from the SEER database, 1973-2005*. Cancer, 2009. **115**(15): p. 3526-36.
29. Brohl, A.S., et al., *The genomic landscape of the Ewing Sarcoma family of tumors reveals recurrent STAG2 mutation*. PLoS Genet, 2014. **10**(7): p. e1004475.

30. Mackintosh, C., et al., *Iq gain and CDT2 overexpression underlie an aggressive and highly proliferative form of Ewing sarcoma*. *Oncogene*, 2012. **31**(10): p. 1287-98.
31. Grünewald, T.G.P., et al., *Ewing sarcoma*. *Nature Reviews Disease Primers*, 2018. **4**(1): p. 5.
32. Riggi, N., et al., *Development of Ewing's sarcoma from primary bone marrow-derived mesenchymal progenitor cells*. *Cancer Res*, 2005. **65**(24): p. 11459-68.
33. Brennan, B., et al., *Comparison of two chemotherapy regimens in patients with newly diagnosed Ewing sarcoma (EE2012): an open-label, randomised, phase 3 trial*. *The Lancet*, 2022. **400**(10362): p. 1513-1521.
34. McCabe, M., et al., *Phase III assessment of topotecan and cyclophosphamide and high-dose ifosfamide in rEECur: An international randomized controlled trial of chemotherapy for the treatment of recurrent and primary refractory Ewing sarcoma (RR-ES)*. *Journal of Clinical Oncology*. **40**(17_suppl): p. LBA2-LBA2.
35. Gaspar, N., et al., *Ewing Sarcoma: Current Management and Future Approaches Through Collaboration*. *J Clin Oncol*, 2015. **33**(27): p. 3036-46.
36. Ginsberg, J.P., et al., *Long-term survivors of childhood Ewing sarcoma: report from the childhood cancer survivor study*. *J Natl Cancer Inst*, 2010. **102**(16): p. 1272-83.
37. Longhi, A., et al., *Late effects of chemotherapy and radiotherapy in osteosarcoma and Ewing sarcoma patients: the Italian Sarcoma Group Experience (1983-2006)*. *Cancer*, 2012. **118**(20): p. 5050-9.
38. Marina, N.M., et al., *Longitudinal follow-up of adult survivors of Ewing sarcoma: A report from the Childhood Cancer Survivor Study*. *Cancer*, 2017. **123**(13): p. 2551-2560.
39. Ohno, T., V.N. Rao, and E.S. Reddy, *EWS/Fli-1 chimeric protein is a transcriptional activator*. *Cancer Res*, 1993. **53**(24): p. 5859-63.
40. Cidre-Aranaz, F. and J. Alonso, *EWS/FLII Target Genes and Therapeutic Opportunities in Ewing Sarcoma*. *Front Oncol*, 2015. **5**: p. 162.
41. Riggi, N., et al., *EWS-FLII utilizes divergent chromatin remodeling mechanisms to directly activate or repress enhancer elements in Ewing sarcoma*. *Cancer Cell*, 2014. **26**(5): p. 668-681.
42. Thelin-Järnum, S., et al., *The myxoid liposarcoma specific TLS-CHOP fusion protein localizes to nuclear structures distinct from PML nuclear bodies*. *Int J Cancer*, 2002. **97**(4): p. 446-50.
43. Hou, X., et al., *FUS::DDIT3 Fusion Protein in the Development of Myxoid Liposarcoma and Possible Implications for Therapy*. 2024. **14**(10): p. 1297.

44. Göransson, M., et al., *The myxoid liposarcoma FUS-DDIT3 fusion oncoprotein deregulates NF- κ B target genes by interaction with NFKBIZ*. *Oncogene*, 2009. **28**(2): p. 270-278.
45. Potratz, J., et al., *Receptor tyrosine kinase gene expression profiles of Ewing sarcomas reveal ROR1 as a potential therapeutic target in metastatic disease*. *Mol Oncol*, 2016. **10**(5): p. 677-92.
46. Negri, T., et al., *Functional Mapping of Receptor Tyrosine Kinases in Myxoid Liposarcoma*. *Clinical Cancer Research*, 2010. **16**(14): p. 3581-3593.
47. Lemmon, M.A. and J. Schlessinger, *Cell Signaling by Receptor Tyrosine Kinases*. *Cell*, 2010. **141**(7): p. 1117-1134.
48. Trautmann, M., et al., *FUS-DDIT3 Fusion Protein-Driven IGF-IR Signaling is a Therapeutic Target in Myxoid Liposarcoma*. *Clin Cancer Res*, 2017. **23**(20): p. 6227-6238.
49. Olofsson, A., et al., *Abnormal expression of cell cycle regulators in FUS-CHOP carrying liposarcomas*. *Int J Oncol*, 2004. **25**(5): p. 1349-55.
50. Sleijfer, S., et al., *Pazopanib, a Multikinase Angiogenesis Inhibitor, in Patients With Relapsed or Refractory Advanced Soft Tissue Sarcoma: A Phase II Study From the European Organisation for Research and Treatment of Cancer–Soft Tissue and Bone Sarcoma Group (EORTC Study 62043)*. *Journal of Clinical Oncology*, 2009. **27**(19): p. 3126-3132.
51. van der Graaf, W.T.A., et al., *Pazopanib for metastatic soft-tissue sarcoma (PALETTE): a randomised, double-blind, placebo-controlled phase 3 trial*. *The Lancet*, 2012. **379**(9829): p. 1879-1886.
52. Mora, J., et al., *Activated growth signaling pathway expression in Ewing sarcoma and clinical outcome*. 2012. **58**(4): p. 532-538.
53. DuBois, S.G., et al., *Randomized Phase III Trial of Ganitumab With Interval-Compressed Chemotherapy for Patients With Newly Diagnosed Metastatic Ewing Sarcoma: A Report From the Children's Oncology Group*. *J Clin Oncol*, 2023. **41**(11): p. 2098-2107.
54. Bozzi, F., et al., *Evidence for activation of KIT, PDGFRalpha, and PDGFRbeta receptors in the Ewing sarcoma family of tumors*. *Cancer*, 2007. **109**(8): p. 1638-45.
55. Do, I., et al., *Protein expression of KIT and gene mutation of c-kit and PDGFRs in Ewing sarcomas*. *Pathol Res Pract*, 2007. **203**(3): p. 127-34.
56. Andersson, M.K. and P. Aman, *Proliferation of Ewing sarcoma cell lines is suppressed by the receptor tyrosine kinase inhibitors gefitinib and vandetanib*. *Cancer Cell Int*, 2008. **8**: p. 1.
57. Mendoza-Naranjo, A., et al., *ERBB4 confers metastatic capacity in Ewing sarcoma*. *EMBO Mol Med*, 2013. **5**(7): p. 1087-102.

58. Chao, J., et al., *Phase II clinical trial of imatinib mesylate in therapy of KIT and/or PDGFR α -expressing Ewing sarcoma family of tumors and desmoplastic small round cell tumors*. *Anticancer Res*, 2010. **30**(2): p. 547-52.
59. Attia, S., et al., *A phase II trial of regorafenib in patients with advanced Ewing sarcoma and related tumors of soft tissue and bone: SARC024 trial results*. *Cancer Med*, 2023. **12**(2): p. 1532-1539.
60. Chugh, R., et al., *Phase II multicenter trial of imatinib in 10 histologic subtypes of sarcoma using a bayesian hierarchical statistical model*. *J Clin Oncol*, 2009. **27**(19): p. 3148-53.
61. Italiano, A., et al., *Cabozantinib in patients with advanced Ewing sarcoma or osteosarcoma (CABONE): a multicentre, single-arm, phase 2 trial*. *The Lancet Oncology*, 2020. **21**(3): p. 446-455.
62. Sellan-Albert, S., et al., *PEMBROCABOSARC: Combination of pembrolizumab and cabozantinib in patients with advanced sarcomas*. *Journal of Clinical Oncology*, 2023. **41**(16_suppl): p. TPS11586-TPS11586.
63. Boczek, E.E., et al., *Conformational processing of oncogenic v-Src kinase by the molecular chaperone Hsp90*. *Proc Natl Acad Sci U S A*, 2015. **112**(25): p. E3189-98.
64. Watanabe, S., et al., *HSP90 inhibition overcomes EGFR amplification-induced resistance to third-generation EGFR-TKIs*. *Thorac Cancer*, 2021. **12**(5): p. 631-642.
65. Fumo, G., et al., *17-Allylamino-17-demethoxygeldanamycin (17-AAG) is effective in down-regulating mutated, constitutively activated KIT protein in human mast cells*. *Blood*, 2004. **103**(3): p. 1078-1084.
66. Bauer, S., et al., *Heat Shock Protein 90 Inhibition in Imatinib-Resistant Gastrointestinal Stromal Tumor*. *Cancer Research*, 2006. **66**(18): p. 9153-9161.
67. Mendoza, M.C., E.E. Er, and J. Blenis, *The Ras-ERK and PI3K-mTOR pathways: cross-talk and compensation*. *Trends Biochem Sci*, 2011. **36**(6): p. 320-8.
68. Hoter, A., M.E. El-Sabban, and H.Y. Naim, *The HSP90 Family: Structure, Regulation, Function, and Implications in Health and Disease*. *Int J Mol Sci*, 2018. **19**(9).
69. Schopf, F.H., M.M. Biebl, and J. Buchner, *The HSP90 chaperone machinery*. *Nature Reviews Molecular Cell Biology*, 2017. **18**(6): p. 345-360.
70. Li, J. and J. Buchner, *Structure, function and regulation of the hsp90 machinery*. *Biomed J*, 2013. **36**(3): p. 106-17.
71. Prodromou, C., et al., *Identification and Structural Characterization of the ATP/ADP-Binding Site in the Hsp90 Molecular Chaperone*. *Cell*, 1997. **90**(1): p. 65-75.

72. Prodromou, C., *Mechanisms of Hsp90 regulation*. Biochem J, 2016. **473**(16): p. 2439-52.
73. Albakova, Z., *HSP90 multi-functionality in cancer*. Front Immunol, 2024. **15**: p. 1436973.
74. Mahalingam, D., et al., *Targeting HSP90 for cancer therapy*. British Journal of Cancer, 2009. **100**(10): p. 1523-1529.
75. Trepel, J., et al., *Targeting the dynamic HSP90 complex in cancer*. Nature Reviews Cancer, 2010. **10**(8): p. 537-549.
76. Grbovic, O.M., et al., *V600E B-Raf requires the Hsp90 chaperone for stability and is degraded in response to Hsp90 inhibitors*. 2006. **103**(1): p. 57-62.
77. Sato, S., N. Fujita, and T. Tsuruo, *Modulation of Akt kinase activity by binding to Hsp90*. Proc Natl Acad Sci U S A, 2000. **97**(20): p. 10832-7.
78. Rastogi, S., et al., *An update on the status of HSP90 inhibitors in cancer clinical trials*. Cell Stress Chaperones, 2024. **29**(4): p. 519-539.
79. Kurokawa, Y., et al., *Pimipib in patients with advanced gastrointestinal stromal tumor (CHAPTER-GIST-301): a randomized, double-blind, placebo-controlled phase III trial*. Annals of Oncology, 2022. **33**(9): p. 959-967.
80. Hoy, S.M., *Pimipib: First Approval*. Drugs, 2022. **82**(13): p. 1413-1418.
81. Wang, T., et al., *Immunohistochemical analysis of expressions of RBL, CDK4, HSP90, cPLA2G4A, and CHMP2B is helpful in distinction between myxofibrosarcoma and myxoid liposarcoma*. Int J Surg Pathol, 2014. **22**(7): p. 589-99.
82. Steinmann, S., et al., *Hsp90 inhibition by AUY922 as an effective treatment strategy against myxoid liposarcoma*. Cancer Lett, 2015. **367**(2): p. 147-56.
83. Pessetto, Z.Y., et al., *In silico and in vitro drug screening identifies new therapeutic approaches for Ewing sarcoma*. Oncotarget, 2017. **8**(3): p. 4079-4095.
84. de Graaff, M.A., et al., *High-Throughput Screening of Myxoid Liposarcoma Cell Lines: Survivin Is Essential for Tumor Growth*. Transl Oncol, 2017. **10**(4): p. 546-554.
85. Martins, A.S., et al., *A pivotal role for heat shock protein 90 in Ewing sarcoma resistance to anti-insulin-like growth factor 1 receptor treatment: in vitro and in vivo study*. Cancer Res, 2008. **68**(15): p. 6260-70.
86. Papetti, M. and I.M. Herman, *Mechanisms of normal and tumor-derived angiogenesis*. Am J Physiol Cell Physiol, 2002. **282**(5): p. C947-70.

87. Elebiyo, T.C., et al., *Reassessing vascular endothelial growth factor (VEGF) in anti-angiogenic cancer therapy*. Cancer Treatment and Research Communications, 2022. **32**: p. 100620.
88. Song, Y., et al., *Effectiveness of bevacizumab in the treatment of metastatic colorectal cancer: a systematic review and meta-analysis*. BMC Gastroenterol, 2024. **24**(1): p. 58.
89. Gridelli, C., et al., *Safety and Efficacy of Bevacizumab Plus Standard-of-Care Treatment Beyond Disease Progression in Patients With Advanced Non-Small Cell Lung Cancer: The AvaALL Randomized Clinical Trial*. JAMA Oncol, 2018. **4**(12): p. e183486.
90. van der Schaft, D.W., et al., *Tumor cell plasticity in Ewing sarcoma, an alternative circulatory system stimulated by hypoxia*. Cancer Res, 2005. **65**(24): p. 11520-8.
91. DuBois, S.G., N. Marina, and J. Glade-Bender, *Angiogenesis and vascular targeting in Ewing sarcoma: a review of preclinical and clinical data*. Cancer, 2010. **116**(3): p. 749-57.
92. Verschraegen, C.F., et al., *Phase IB study of the combination of docetaxel, gemcitabine, and bevacizumab in patients with advanced or recurrent soft tissue sarcoma: the Axtell regimen*. Annals of Oncology, 2012. **23**(3): p. 785-790.
93. Hanahan, D., *Hallmarks of Cancer: New Dimensions*. Cancer Discovery, 2022. **12**(1): p. 31-46.
94. Shi, J., et al., *The concurrence of DNA methylation and demethylation is associated with transcription regulation*. Nature Communications, 2021. **12**(1): p. 5285.
95. Zhao, Z. and A. Shilatifard, *Epigenetic modifications of histones in cancer*. Genome Biology, 2019. **20**(1): p. 245.
96. Kadoch, C. and G.R. Crabtree, *Mammalian SWI/SNF chromatin remodeling complexes and cancer: Mechanistic insights gained from human genomics*. Sci Adv, 2015. **1**(5): p. e1500447.
97. Michel, B.C., et al., *A non-canonical SWI/SNF complex is a synthetic lethal target in cancers driven by BAF complex perturbation*. Nat Cell Biol, 2018. **20**(12): p. 1410-1420.
98. Donati, B., E. Lorenzini, and A. Ciarrocchi, *BRD4 and Cancer: going beyond transcriptional regulation*. Mol Cancer, 2018. **17**(1): p. 164.
99. Jang, M.K., et al., *The bromodomain protein Brd4 is a positive regulatory component of P-TEFb and stimulates RNA polymerase II-dependent transcription*. Mol Cell, 2005. **19**(4): p. 523-34.
100. Wilson, B.G., et al., *Epigenetic Antagonism between Polycomb and SWI/SNF Complexes during Oncogenic Transformation*. Cancer Cell, 2010. **18**(4): p. 316-328.

101. Kadoch, C., R.A. Copeland, and H. Keilhack, *PRC2 and SWI/SNF Chromatin Remodeling Complexes in Health and Disease*. *Biochemistry*, 2016. **55**(11): p. 1600-1614.
102. Nacev, B.A., et al., *The epigenomics of sarcoma*. *Nat Rev Cancer*, 2020. **20**(10): p. 608-623.
103. Sheffield, N.C., et al., *DNA methylation heterogeneity defines a disease spectrum in Ewing sarcoma*. *Nat Med*, 2017. **23**(3): p. 386-395.
104. Chen, Y., et al., *Bromodomain and extraterminal proteins foster the core transcriptional regulatory programs and confer vulnerability in liposarcoma*. *Nature Communications*, 2019. **10**(1): p. 1353.
105. Lindén, M., et al., *FET fusion oncoproteins interact with BRD4 and SWI/SNF chromatin remodelling complex subtypes in sarcoma*. *Mol Oncol*, 2022.
106. Gollavilli, P.N., et al., *EWS/ETS-Driven Ewing Sarcoma Requires BET Bromodomain Proteins*. *Cancer Res*, 2018. **78**(16): p. 4760-4773.
107. Richter, G.H., et al., *EZH2 is a mediator of EWS/FLI1 driven tumor growth and metastasis blocking endothelial and neuro-ectodermal differentiation*. *Proc Natl Acad Sci U S A*, 2009. **106**(13): p. 5324-9.
108. Wang, J., et al., *Prospects for Epigenetic Targeted Therapies of Bone and Soft-Tissue Sarcomas*. *Sarcoma*, 2021. **2021**: p. 5575444.
109. Hussein, M., et al., *Imaging recommendations for soft-tissue sarcomas: model guidelines from diagnosis to post-treatment follow-up*. *Clinical Radiology*, 2024. **79**(12): p. 881-891.
110. Rothermundt, C., et al., *What is the role of routine follow-up for localised limb soft tissue sarcomas? A retrospective analysis of 174 patients*. *Br J Cancer*, 2014. **110**(10): p. 2420-6.
111. Richardson, M.L., et al., *MR characterization of post-irradiation soft tissue edema*. *Skeletal Radiol*, 1996. **25**(6): p. 537-43.
112. Cao, C.-F., et al., *CT Scans and Cancer Risks: A Systematic Review and Dose-response Meta-analysis*. *BMC Cancer*, 2022. **22**(1): p. 1238.
113. Zhou, Y., et al., *Tumor biomarkers for diagnosis, prognosis and targeted therapy*. *Signal Transduction and Targeted Therapy*, 2024. **9**(1): p. 132.
114. Fujibuchi, T., et al., *Serum lactate dehydrogenase levels predict the prognosis of patients with soft tissue sarcoma*. *Mol Clin Oncol*, 2022. **16**(3): p. 65.
115. Alix-Panabières, C. and K. Pantel, *Clinical applications of circulating tumor cells and circulating tumor DNA as liquid biopsy*. *Cancer Discovery*, 2016. **6**(5): p. 479-491.
116. Bartolomucci, A., et al., *Circulating tumor DNA to monitor treatment response in solid tumors and advance precision oncology*. *npj Precision Oncology*, 2025. **9**(1): p. 84.

117. Kim, H. and K.U. Park, *Clinical Circulating Tumor DNA Testing for Precision Oncology*. *Cancer Res Treat*, 2023. **55**(2): p. 351-366.
118. Wang, Y.-H., et al., *Circulating tumor DNA analysis for tumor diagnosis*. *Talanta*, 2021. **228**: p. 122220.
119. Eisenhardt, A.E., et al., *Targeted next-generation sequencing of circulating free DNA enables non-invasive tumor detection in myxoid liposarcomas*. *Mol Cancer*, 2022. **21**(1): p. 50.
120. Schmid, A., et al., *Improved Quantification of Circulating Tumor DNA in Translocation-Associated Myxoid Liposarcoma by Simultaneous Detection of Breakpoints and Single Nucleotide Variants*. 2025. **14**(4): p. e70704.
121. Shulman, D.S., et al., *Detection of circulating tumour DNA is associated with inferior outcomes in Ewing sarcoma and osteosarcoma: a report from the Children's Oncology Group*. *British Journal of Cancer*, 2018. **119**(5): p. 615-621.
122. Seidel, M.G., et al., *Clinical implementation of plasma cell-free circulating tumor DNA quantification by digital droplet PCR for the monitoring of Ewing sarcoma in children and adolescents*. 2022. **Volume 10 - 2022**.
123. Di Sario, G., et al., *Enhancing clinical potential of liquid biopsy through a multi-omic approach: A systematic review*. *Front Genet*, 2023. **14**: p. 1152470.
124. Voloshin, N., et al., *Practical Use of Immortalized Cells in Medicine: Current Advances and Future Perspectives*. *Int J Mol Sci*, 2023. **24**(16).
125. Mirabelli, P., L. Coppola, and M. Salvatore, *Cancer Cell Lines Are Useful Model Systems for Medical Research*. *Cancers (Basel)*, 2019. **11**(8).
126. Åman, P., et al., *Rearrangement of the transcription factor gene CHOP in myxoid liposarcomas with t(12;16)(q13;p11)*. *Genes Chromosom Cancer*, 1992. **5**(4): p. 278-285.
127. Thelin-Järnum, S., et al., *Identification of genes differentially expressed in TLS-CHOP carrying myxoid liposarcomas*. *Int J Cancer*, 1999. **83**(1): p. 30-3.
128. Engström, K., et al., *The myxoid/round cell liposarcoma fusion oncogene FUS-DDIT3 and the normal DDIT3 induce a liposarcoma phenotype in transfected human fibrosarcoma cells*. *Am J Pathol*, 2006. **168**(5): p. 1642-53.
129. Whang-Peng, J., et al., *Chromosome translocation in peripheral neuroepithelioma*. *N Engl J Med*, 1984. **311**(9): p. 584-5.
130. Whang-Peng, J., et al., *Cytogenetic characterization of selected small round cell tumors of childhood*. *Cancer Genet Cytogenet*, 1986. **21**(3): p. 185-208.

131. Qin, J., et al., *Biological characteristics and immune responses of NK Cells in commonly used experimental mouse models*. Front Immunol, 2024. **15**: p. 1478323.
132. Vladutiu, A.O., *The severe combined immunodeficient (SCID) mouse as a model for the study of autoimmune diseases*. Clin Exp Immunol, 1993. **93**(1): p. 1-8.
133. O'Brien, J., et al., *Investigation of the Alamar Blue (resazurin) fluorescent dye for the assessment of mammalian cell cytotoxicity*. Eur J Biochem, 2000. **267**(17): p. 5421-6.
134. Sebaugh, J.L., *Guidelines for accurate EC50/IC50 estimation*. Pharm Stat, 2011. **10**(2): p. 128-34.
135. Zhang, Y. and R.L. Judson, *Evaluation of holographic imaging cytometer holomonitor M4® motility applications*. Cytometry A, 2018. **93**(11): p. 1125-1131.
136. Ianevski, A., et al., *SynergyFinder: a web application for analyzing drug combination dose-response matrix data*. Bioinformatics, 2017. **33**(15): p. 2413-2415.
137. Ianevski, A., A.K. Giri, and T. Aittokallio, *SynergyFinder 3.0: an interactive analysis and consensus interpretation of multi-drug synergies across multiple samples*. Nucleic Acids Res, 2022. **50**(W1): p. W739-w743.
138. Yadav, B., et al., *Searching for Drug Synergy in Complex Dose-Response Landscapes Using an Interaction Potency Model*. Comput Struct Biotechnol J, 2015. **13**: p. 504-13.
139. El Khili, M.R., S.A. Memon, and A. Emad, *MARSY: a multitask deep-learning framework for prediction of drug combination synergy scores*. Bioinformatics, 2023. **39**(4).
140. Malyutina, A., et al., *Drug combination sensitivity scoring facilitates the discovery of synergistic and efficacious drug combinations in cancer*. PLoS Comput Biol, 2019. **15**(5): p. e1006752.
141. Livak, K.J. and T.D. Schmittgen, *Analysis of Relative Gene Expression Data Using Real-Time Quantitative PCR and the 2- $\Delta\Delta$ CT Method*. Methods, 2001. **25**(4): p. 402-408.
142. Toki, M.I., et al., *Proof of the quantitative potential of immunofluorescence by mass spectrometry*. Laboratory Investigation, 2017. **97**(3): p. 329-334.
143. Bankhead, P., et al., *QuPath: Open source software for digital pathology image analysis*. Scientific Reports, 2017. **7**(1): p. 16878.
144. Eisenhauer, E.A., et al., *New response evaluation criteria in solid tumours: revised RECIST guideline (version 1.1)*. 2009. **45**(2): p. 228-247.

145. Prasad, S.R. and S. Saini, *Radiological evaluation of oncologic treatment response: current update*. Cancer Imaging, 2003. **3**(2): p. 93-95.
146. Goldmacher, G.V. and J. Conklin, *The use of tumour volumetrics to assess response to therapy in anticancer clinical trials*. Br J Clin Pharmacol, 2012. **73**(6): p. 846-54.
147. Stahlberg, A., et al., *Simple, multiplexed, PCR-based barcoding of DNA enables sensitive mutation detection in liquid biopsies using sequencing*. Nucleic Acids Res, 2016. **44**(11): p. e105.
148. Österlund, T., et al., *UMIErrorCorrect and UMIAnalyzer: Software for Consensus Read Generation, Error Correction, and Visualization Using Unique Molecular Identifiers*. Clin Chem, 2022. **68**(11): p. 1425-1435.
149. Lundberg, M., et al., *Homogeneous antibody-based proximity extension assays provide sensitive and specific detection of low-abundant proteins in human blood*. Nucleic Acids Research, 2011. **39**(15): p. e102-e102.
150. Eldjarn, G.H., et al., *Large-scale plasma proteomics comparisons through genetics and disease associations*. Nature, 2023. **622**(7982): p. 348-358.
151. Assarsson, E., et al., *Homogenous 96-plex PEA immunoassay exhibiting high sensitivity, specificity, and excellent scalability*. PLoS One, 2014. **9**(4): p. e95192.
152. Alfano, L., et al., *RET is a heat shock protein 90 (HSP90) client protein and is knocked down upon HSP90 pharmacological block*. J Clin Endocrinol Metab, 2010. **95**(7): p. 3552-7.
153. Zuehlke, A. and J.L. Johnson, *Hsp90 and co-chaperones twist the functions of diverse client proteins*. Biopolymers, 2010. **93**(3): p. 211-7.
154. Li, L., et al., *An updated patent review of anticancer Hsp90 inhibitors (2013-present)*. Expert Opinion on Therapeutic Patents, 2021. **31**(1): p. 67-80.
155. Miyajima, N., et al., *The HSP90 inhibitor ganetespib synergizes with the MET kinase inhibitor crizotinib in both crizotinib-sensitive and -resistant MET-driven tumor models*. Cancer Res, 2013. **73**(23): p. 7022-33.
156. Lin, S.-F., et al., *Efficacy of an HSP90 inhibitor, ganetespib, in preclinical thyroid cancer models*. 2017. **8**(25).
157. Joensuu, H. and S. Dimitrijevic, *Tyrosine kinase inhibitor imatinib (STI571) as an anticancer agent for solid tumours*. Ann Med, 2001. **33**(7): p. 451-5.

158. Javidi-Sharifi, N., et al., *Crosstalk between KIT and FGFR3 Promotes Gastrointestinal Stromal Tumor Cell Growth and Drug Resistance*. *Cancer Res*, 2015. **75**(5): p. 880-91.
159. Li, Y. and E. Seto, *HDACs and HDAC Inhibitors in Cancer Development and Therapy*. Cold Spring Harb Perspect Med, 2016. **6**(10).
160. Welch, D., et al., *Small molecule inhibition of lysine-specific demethylase 1 (LSD1) and histone deacetylase (HDAC) alone and in combination in Ewing sarcoma cell lines*. *PLoS One*, 2019. **14**(9): p. e0222228.
161. Laubach, J.P., et al., *Efficacy and safety of oral panobinostat plus subcutaneous bortezomib and oral dexamethasone in patients with relapsed or relapsed and refractory multiple myeloma (PANORAMA 3): an open-label, randomised, phase 2 study*. *The Lancet Oncology*, 2021. **22**(1): p. 142-154.
162. Bjursten, S., et al., *Response to BRAF/MEK Inhibition in A598_T599insV BRAF Mutated Melanoma*. *Case Rep Oncol*, 2019. **12**(3): p. 872-879.
163. Vannas, C., et al., *Dynamic ctDNA evaluation of a patient with BRAFV600E metastatic melanoma demonstrates the utility of ctDNA for disease monitoring and tumor clonality analysis*. *Acta Oncol*, 2020: p. 1-5.
164. Micallef, P., et al., *Digital sequencing is improved by using structured unique molecular identifiers*. *Genome Biology*, 2025. **26**(1): p. 37.
165. Vannas, C., et al., *Treatment Monitoring of a Patient with Synchronous Metastatic Angiosarcoma and Breast Cancer Using ctDNA*. *International Journal of Molecular Sciences*, 2024. **25**(7).
166. Doroshow, D.B., et al., *PD-L1 as a biomarker of response to immune-checkpoint inhibitors*. *Nat Rev Clin Oncol*, 2021. **18**(6): p. 345-362.
167. Mahoney, K.M., et al., *Soluble PD-L1 as an early marker of progressive disease on nivolumab*. *Journal for ImmunoTherapy of Cancer*, 2022. **10**(2): p. e003527.
168. Oh, S.Y., et al., *Soluble PD-L1 is a predictive and prognostic biomarker in advanced cancer patients who receive immune checkpoint blockade treatment*. *Scientific Reports*, 2021. **11**(1): p. 19712.
169. Scirocchi, F., et al., *Soluble PD-L1 as a Prognostic Factor for Immunotherapy Treatment in Solid Tumors: Systematic Review and Meta-Analysis*. *Int J Mol Sci*, 2022. **23**(22).
170. Burgess, M.A., et al., *Clinical activity of pembrolizumab (P) in undifferentiated pleomorphic sarcoma (UPS) and dedifferentiated/pleomorphic liposarcoma (LPS): Final results of*

- SARC028 expansion cohorts*. Journal of Clinical Oncology. **37**(15_suppl): p. 11015-11015.
171. Min, H.-Y. and H.-Y. Lee, *Molecular targeted therapy for anticancer treatment*. Experimental & Molecular Medicine, 2022. **54**(10): p. 1670-1694.
 172. Demetri, G.D., et al., *Efficacy and Safety of Imatinib Mesylate in Advanced Gastrointestinal Stromal Tumors*. 2002. **347**(7): p. 472-480.
 173. Fu, K., et al., *Therapeutic strategies for EGFR-mutated non-small cell lung cancer patients with osimertinib resistance*. Journal of Hematology & Oncology, 2022. **15**(1): p. 173.
 174. Larkin, J., et al., *Five-Year Survival with Combined Nivolumab and Ipilimumab in Advanced Melanoma*. 2019. **381**(16): p. 1535-1546.
 175. Liu, Y., et al., *Multi-omic measurements of heterogeneity in HeLa cells across laboratories*. Nature Biotechnology, 2019. **37**(3): p. 314-322.
 176. Ben-David, U., et al., *Genetic and transcriptional evolution alters cancer cell line drug response*. Nature, 2018. **560**(7718): p. 325-330.
 177. Gengenbacher, N., M. Singhal, and H.G. Augustin, *Preclinical mouse solid tumour models: status quo, challenges and perspectives*. Nature Reviews Cancer, 2017. **17**(12): p. 751-765.
 178. Brown, J.M., et al., *Genetically engineered mouse model of pleomorphic liposarcoma: Immunophenotyping and histologic characterization*. Neoplasia, 2024. **48**: p. 100956.
 179. Chen, M., et al., *The Fusion Oncogene FUS-CHOP Drives Sarcomagenesis of High-Grade Spindle Cell Sarcomas in Mice*. Sarcoma, 2019. **2019**: p. 1340261.
 180. Charytonowicz, E., et al., *PPAR γ agonists enhance ET-743-induced adipogenic differentiation in a transgenic mouse model of myxoid round cell liposarcoma*. The Journal of Clinical Investigation, 2012. **122**(3): p. 886-898.
 181. Tanaka, M. and T. Nakamura, *Genetically Engineered Mouse Model in Ewing Sarcoma*. Methods Mol Biol, 2021. **2226**: p. 183-189.
 182. Nakahata, K., et al., *K-Ras and p53 mouse model with molecular characteristics of human rhabdomyosarcoma and translational applications*. Dis Model Mech, 2022. **15**(2).
 183. Gustafsson, A., et al., *Patient-derived scaffolds as a drug-testing platform for endocrine therapies in breast cancer*. Scientific Reports, 2021. **11**(1): p. 13334.
 184. Ranji, P., et al., *Deciphering the role of FUS::DDIT3 expression and tumor microenvironment in myxoid liposarcoma development*. Journal of Translational Medicine, 2024. **22**(1).
 185. Sun, D., et al., *Why 90% of clinical drug development fails and how to improve it?* Acta Pharm Sin B, 2022. **12**(7): p. 3049-3062.

186. Chan, S.P.Y., et al., *Functional combinatorial precision medicine for predicting and optimizing soft tissue sarcoma treatments*. npj Precision Oncology, 2025. **9**(1): p. 83.
187. Békés, M., D.R. Langley, and C.M. Crews, *PROTAC targeted protein degraders: the past is prologue*. Nature Reviews Drug Discovery, 2022. **21**(3): p. 181-200.
188. Dai, W., et al., *Epigenetics-targeted drugs: current paradigms and future challenges*. Signal Transduction and Targeted Therapy, 2024. **9**(1): p. 332.
189. Hoy, S.M., *Tazemetostat: First Approval*. Drugs, 2020. **80**(5): p. 513-521.
190. Knutson, S.K., et al., *Durable tumor regression in genetically altered malignant rhabdoid tumors by inhibition of methyltransferase EZH2*. 2013. **110**(19): p. 7922-7927.
191. Hollmann, T.J. and J.L. Hornick, *INI1-Deficient Tumors: Diagnostic Features and Molecular Genetics*. 2011. **35**(10): p. e47-e63.
192. Gong, H., et al., *Targeted Therapy for EWS-FLI1 in Ewing Sarcoma*. 2023. **15**(16): p. 4035.
193. Nabet, B., et al., *Rapid and direct control of target protein levels with VHL-recruiting dTAG molecules*. Nat Commun, 2020. **11**(1): p. 4687.
194. Erkizan, H.V., et al., *A small molecule blocking oncogenic protein EWS-FLI1 interaction with RNA helicase A inhibits growth of Ewing's sarcoma*. Nat Med, 2009. **15**(7): p. 750-6.
195. Ludwig, J.A., et al., *TK216 for relapsed/refractory Ewing sarcoma: Interim phase 1/2 results*. 2021. **39**(15_suppl): p. 11500-11500.
196. Povedano, J.M., et al., *TK216 targets microtubules in Ewing sarcoma cells*. Cell Chemical Biology, 2022. **29**(8): p. 1325-1332.e4.
197. Grohar, P.J., et al., *Ecteinascidin 743 interferes with the activity of EWS-FLI1 in Ewing sarcoma cells*. Neoplasia, 2011. **13**(2): p. 145-53.
198. Forni, C., et al., *Trabectedin (ET-743) promotes differentiation in myxoid liposarcoma tumors*. Mol Cancer Ther, 2009. **8**(2): p. 449-57.
199. Craparotta, I., et al., *Mechanism of efficacy of trabectedin against myxoid liposarcoma entails detachment of the FUS-DDIT3 transcription factor from its DNA binding sites*. J Exp Clin Cancer Res, 2024. **43**(1): p. 309.
200. Gronchi, A., et al., *Phase II clinical trial of neoadjuvant trabectedin in patients with advanced localized myxoid liposarcoma*. Ann Oncol, 2012. **23**(3): p. 771-776.
201. Grosso, F., et al., *Trabectedin in myxoid liposarcomas (MLS): a long-term analysis of a single-institution series*. Ann Oncol, 2009. **20**(8): p. 1439-44.

202. Takahashi, M., et al., *Efficacy of Trabectedin in Patients with Advanced Translocation-Related Sarcomas: Pooled Analysis of Two Phase II Studies*. *Oncologist*, 2017. **22**(8): p. 979-988.
203. Demetri, G.D., et al., *Efficacy and Safety of Trabectedin or Dacarbazine for Metastatic Liposarcoma or Leiomyosarcoma After Failure of Conventional Chemotherapy: Results of a Phase III Randomized Multicenter Clinical Trial*. *J Clin Oncol*, 2016. **34**(8): p. 786-93.
204. Baruchel, S., et al., *A phase 2 trial of trabectedin in children with recurrent rhabdomyosarcoma, Ewing sarcoma and non-rhabdomyosarcoma soft tissue sarcomas: a report from the Children's Oncology Group*. 2012. **48**(4): p. 579-585.
205. Zer, A., et al., *Multi-agent chemotherapy in advanced soft tissue sarcoma (STS) – A systematic review and meta-analysis*. *Cancer Treatment Reviews*, 2018. **63**: p. 71-78.
206. Verma, S., et al., *Meta-analysis of ifosfamide-based combination chemotherapy in advanced soft tissue sarcoma*. *Cancer Treat Rev*, 2008. **34**(4): p. 339-47.
207. Zhang, T., et al., *Efficacy Comparison of Six Chemotherapeutic Combinations for Osteosarcoma and Ewing's Sarcoma Treatment: A Network Meta-Analysis*. *J Cell Biochem*, 2018. **119**(1): p. 250-259.
208. Tie, J., et al., *Circulating Tumor DNA Analysis Guiding Adjuvant Therapy in Stage II Colon Cancer*. 2022. **386**(24): p. 2261-2272.
209. Huang, J., et al., *Circulating IL6 is involved in the infiltration of M2 macrophages and CD8+ T cells*. *Sci Rep*, 2025. **15**(1): p. 8681.

APPENDIX

Appendix 1

72-75

Reprint: Vannas, C. *Vad kan analyser av cellfritt tumör-DNA bidra med?* Onkologi i Sverige, 2019: 1.

Appendix 2

76-81

Reprint: Lindén, M. and Vannas, C. *Okänd interaktion bakom genombrott i förståelsen av hur vissa sarkom uppstår.* Onkologi i Sverige, 2019: 4.

Appendix 3

82-85

Reprint: Vannas, C. *Rapport från Lynn Sages bröstcancersymposium i Chicago.* Cancerläkaren, 2025: 1.